A Lagrangian Perspective of the Hydrological Cycle in the Congo River Basin

Rogert Sorí[1], Raquel Nieto[1,2], Sergio M. Vicente-Serrano[3], Anita Drumond[1], Luis Gimeno[1]

[1] Environmental Physics Laboratory (EphysLab), Universidade de Vigo, Ourense, 32004, Spain
[2] Department of Atmospheric Sciences, Institute of Astronomy, Geophysics and Atmospheric Sciences, University of SãoPaulo, São Paulo, 05508-090, Brazil
[3] Instituto Pirenaico de Ecología, Consejo Superior de Investigaciones Científicas (IPE-CSIC), Zaragoza, 50059, Spain

Correspondence to: Rogert Sorí (rogert.sori@uvigo.es)

Abstract.

The Lagrangian model FLEXPART was used to identify the moisture sources of the Congo River Basin (CRB) and investigate their role in the hydrological cycle. This model allows us to track atmospheric parcels while calculating changes in the specific humidity through the budget of evaporation-minus-precipitation. The method permitted the identification at an annual scale of five continental and four oceanic regions that provide moisture to the CRB from both hemispheres over the course of the year. The most important is the CRB itself, providing more than 50% of the total atmospheric moisture income to the basin. Apart from this, both the land extension to the east of the CRB together with the ocean located in the eastern equatorial South Atlantic Ocean are also very important sources, while the Red Sea source is merely important in the budget of *(E-P)* over the CRB, despite its high evaporation rate. The moisture sink patterns over the CRB in air masses tracked forwards from all the sources follow the latitudinal rainfall migration and are mostly highly correlated with the pattern of precipitation rate, ensuring a link between them. In wet (dry) years the contribution of moisture to precipitation from the CRB over itself increases (decreases). Particularly in dry years, despite to the enhanced evaporative conditions over the basin, the vertically integrated moisture flux (VIMF) divergence inhibit the precipitation and suggest the transport of moisture from the CRB to remote regions.

1 Introduction

The water falling on a given area as precipitation may have been supplied to it by local evaporation and/or transpiration, alternatively, it may have been advected from a remote terrestrial source, or it may have originated in evaporation from the oceans (Dirmeyer, 1999). In recent years, a great number of studies have focused on deepening our understanding of these issues, particularly the mechanisms of water vapour transport in the atmosphere and the identification of moisture sources. These issues are considered some of the major challenges in the atmospheric sciences (Gimeno et al., 2013a). Several techniques and methods have been implemented in an attempt to address these matters; a summary of the main strengths and weaknesses of each was provided by Gimeno et al. (2012).

In respect of Africa in particular, some authors have investigated the sources of moisture for the whole continent (van der Ent., 2010; Gimeno et al., 2010, 2012), and specific regions such as the Sahel (Nieto et al., 2006; Salih et al., 2015; Keys et al., 2012, 2014), Ethiopia (Viste and Sorteberg, 2013), and the wider region of West Africa (Savenije, 1995; Eltahir and Gong, 1996; Druyan and Koster, 1989). Nevertheless, the Congo River Basin (CRB), in the highly convective region of Central Equatorial Africa (CEA), is one of the least studied of the major global river basins (Alsdorf et al., 2016). Focusing on several world river catchments including the Congo, Stohl and James (2005) used the Lagrangian model FLEXPART over a period of 4 years (Dec 1999 - Nov 2003) to diagnose the net budget of *(E-P)*, where *(E)* denotes evaporation and *(P)* precipitation. However, the short time-scale involved in this study was not sufficient to investigate properly the variability and other aspects of the hydrological cycle over the CRB. Gimeno et al. (2010) argued that in tropical South Africa during the austral winter the rate of evaporation is so high that it provides moisture for most of the precipitation over the Congo, and besides this according to van der Ent et al. (2010), the moisture that evaporates in East Africa is the main source of rainfall in the CRB.

More accurate results on the evaporative moisture sources for the CRB, together with their seasonal variations and mean contributions over a period of 25 years, are available online from the Center for Ocean-Land-Atmosphere Studies (COLA). These were calculated using a Quasi-Isentropic method, an Eulerian approach implemented in Dirmeyer et al. (2009), and the results highlight that the main evaporative sources for precipitation lie within the basin itself, in addition to the land to the east of the basin along the oriental African coasts, and the Atlantic and Indian Oceans. However, it is not yet clear what the role of the CRB moisture sources is in other stages of the hydrological cycle and during extreme events in the basin. Most of the studies based on instrumental records in Africa indicate that droughts have become more frequent, intense and widespread during the last 50 years (Dai, 2013; Masih et al., 2014). The occurrence of drought is especially important in regions where economic activities are highly dependent on water resources (like the CRB), and particularly affect those African nations that are heavily reliant on agriculture (Lobell et al., 2011a, b).

The objectives of this study are: i) to identify the main continental and oceanic moisture sources for the CRB from a Lagrangian perspective and determine their role, including that of the basin itself in the total moisture influx to the basin, and ii) to investigate drought and wet conditions in the CRB and the relationship of these to atmospheric moisture influx.

1.1 Region of Study

The Congo River Basin (CRB) is located in central-equatorial Africa, an important part of the continent containing major rivers and dense forest (Fig. 1). With an approximate area of 3,687,000 km^2 (Alsdorf et al., 2016), the basin includes several African countries: the Democratic Republic of the Congo (DRC), the People's Republic of the Congo, the Central African Republic, and parts of Zambia, Angola, Cameroon, and Tanzania (Chishugi, 2008). The Congo River (also known as the Zaire during at one time) is over 4,375 km long, considered to be the fifth longest river in the world, and the second longest in Africa after the Nile River (IBP, 2015). Its discharge shows a composite variability, which is due to the sum of its

tributaries (Laraque 2001). With an annual discharge of 5000 $m^3 s^{-1}$ at its mouth, the Oubangui River is the second most important tributary to the Congo River (mean flow 41 000 $m^3 s^{-1}$), after the Kasai River (8000 $m^3 s^{-1}$) (Briquet, 1995).

The CRB comprises the second largest continuous rainforest in the world; covering an area of approximately 1.8 Million km^2 the high rate of evaporation is comparable to the oceans is one of the main features of the forests, being extremely important for storing carbon and having an impact on the continental and global climate system mainly through the water cycle (Haensler et al., 2013; Marquant et al., 2015; Wasseige et al. 2015). The basin is composed basically of a central area that contains an immense forest swamp best known as "Cuvette Centrale"; an immense depression at the centre of the basin where sediment accumulation since the Quaternary alluvial deposits rest on thick sediments of continental origin, consisting principally of sands and sandstones (Kadima et al., 2011; Gana and Herbert, 2014) (Fig. 1). Here the spatial distribution of forested wetland types is controlled by topography and also by the time and the intensity of the submersion, making it the most extensive peatland complex in the tropics (Dargie et al., 2017). From a rainfall point of view, because of the topographic barrier around the "Cuvette Centrale", the Congolese central basin functions to a large extent as a closed system of precipitation, on-site evaporation, and precipitation (Robert, 1946; Sorre, 1948). Located in the heart of the dense Congolese equatorial forest is the Lake Telé, an immense elliptical body of water (3 m deep for a surface of 23 km^2 and a maximum water storage evaluated to $55x10^6 m^3$) where hydrological exchanges are almost exclusively vertical with very little lateral contribution from the surrounding swamp (Lareque et al., 1998). Furthermore, the basin contains several large, permanent open water lakes including Lake Tanganyika, the largest of the African rift lakes and the world's second largest by volume and depth (Coulter, 1991; Cohen et al., 1993).

Around the central basin, there is mainly a humid evergreen dense forest and to the north and south mosaics of mixed forest; woody savannahs savannas and savannas (Marquant et al., 2015). The current distributions of different forest types correlate strongly with annual rainfall and particularly with the length and severity of dry seasons (CARPE, 2005). The CRB moist forests are the continent's main forest resource, containing an extraordinary biodiversity (Ilumbe, 2006; SCBD-CAFC, 2009) that brings important economic benefits to approximately 60 million people living in local communities (Hugues, 2011; Marquant et al., 2015). Unfortunately, in the CRB the rate of deforestation varies from one country to another. Overall, the basin had a net deforestation rate of 0.09% between 1990 and 2000, compared with 0.17% between 2000 and 2005 (Tchatchou et al., 2015). In fact, the satellite data show a widespread decline in greenness in the northern Congolese forest over the past decade, which is generally consistent with decreases in rainfall, terrestrial water storage, and other related aspects (Potapov et al., 2012; Zhou et al., 2014; Hua et al., 2016) like hydrological regimes (Laraque et al., 2001; Laraque et al., 2013; Wesselink, 1996).

The air masses originating from three permanent anticyclones located to the north-west (Azores), south-west (St. Helena), and south-east (Mascarene) of the CRB converge along the Intertropical Convergence Zone (ITCZ), which separates the

southerly low-level winds from the northerly winds, and the Inter-Oceanic Confluence Zone (IOCZ), separating the westerly from the easterly winds in the southern part of Africa (Samba and Nganga, 2012). In general two modes of circulation: circulation of Hadley and the Walker circulation control the movement of air masses and the climate in Central Africa, leading to moisture convergence not being uniform in the atmospheric column (Tsalefac et al., 2015, Pokam et al., 2012). Areas which are positively correlated with Congo convection are areas of the ascending arm of the Hadley cell (Matari, 2002), while the east-west oscillation of the Walker circulation cell modulates the moisture advection from the Atlantic Ocean and the upward motion over the CRB (Matari, 2002; Lau and Yang, 2002). The rainfall-generating mechanisms are controlled by a zone of shallow depression systems in the CRB (Samba and Nganga, 2012) as well as north-south ITCZ migration (Samba and Nganga, 2012; Alsdorf et al., 2016) together with Mesoscale Convective Systems (MCS) (Jackson et al., 2009) and the African Easterly Jet along with the typical circulation of the Hadley cell (Nicholson, 2009; Pokam et al., 2012; Haensler et al., 2013).

2 Data and Methodology

The drainage area of the Congo River Basin (CRB) (Fig. 1) was defined using geo-referenced watershed boundaries on a 30 arc-second resolution map (a Hydrobasin product of HydroSHEDS (Hydrological data and maps based on SHuttle Elevation Derivatives at multiple Scales), Lehner and Grill (2013)). This was used to obtain the spatial mask of the basin, which was later implemented in the computations.

The methodology implemented here is based on the Lagrangian model FLEXPART developed by Stohl and James (2004, 2005). The model allows us to track the parcels backwards and forwards; thus the model outputs were used to compute the gain and loss of humidity along trajectories of air particles leaving and arriving in the CRB. The backward analysis was utilized for the identification of the moisture sources for the CRB and the forward to obtain their climatological moisture supply and the relationship with the precipitation on it. The approach implemented here has been widely and successfully applied to study the atmospheric branch of the hydrological cycle (e.g., Stohl and James, 2004, 2005; Nieto et al., 2008; Gimeno et al., 2010; Gimeno et al., 2012; Chen et al., 2012; Viste and Sorteberg, 2013; Drumond et al., 2014).

In this method, the atmosphere is divided into N evenly distributed “particles” or “parcels”, whose advection is described by Eq. (1):

$$dx/dt = v\,[x(t)], \tag{1}$$

where x is the position of the parcel and $v\,[x(t)]$ is the wind speed interpolated in space and time. The gain (through evaporation from the environment e) or loss (through precipitation p) of specific humidity (q) by each parcel is calculated following Eq. (2). Along individual trajectories q fluctuations can occur for nonphysical reasons (e.g., because of q interpolation or trajectory errors), a limitation partly compensated by the presence of so many particles in an atmospheric column over the target area, thus:

$$(e - p) = m(dq/dt), \tag{2}$$

where additionally m is the mass of a particle. By integrating over an area of interest it is possible to obtain the net effect of the moisture changes in all the particles in the atmospheric column and, as a consequence, a diagnosis of the surface freshwater flux, hereafter represented by *(E-P)* (Stohl and James, 2004). It is worth mentioning that in some regions atmospheric moisture is not precipitated but just flows through; while in others the convergence of moisture ensures that precipitation occurs (Pokam et al., 2012). A region is then considered a moisture source when *(E-P)>0*, and the net moisture budget of the particles tracked is favourable to evaporation from the environment to the particles. In moisture sink regions the opposite occurs, i.e., the associated moisture budget is favourable to moisture loss from the tracked particles to the environment. A analysis backwards in time tells us where the atmospheric moisture in the air masses over the CRB came from, enabling us to identify the main oceanic and continental sources of moisture. The analysis was applied for 10 days, which is the average residence time of water vapour in the atmosphere (hereafter we use *(E-P)i10*) (Eltahir and Bras, 1996; Numaguti, 1999).

The Lagrangian data used in this work were obtained from a FLEXPART v9.0 experiment executed on a global domain, in which the atmosphere was divided into about 2.0 million uniformly distributed particles. FLEXPART uses ERA-Interim reanalysis data (Dee et al., 2011) available at 6 h intervals (00, 06, 12, and 18 UTC) at a resolution of 1° at 61 vertical levels, from 0.1 to 1000 hPa, with approximately 14 model levels below 1500 m and 23 below 5000 m. This is important because the transport of water vapour occurs mainly in the lower troposphere, which is clearly affected by the earth's topography (Peixoto and Oort, 1992).

To ensure the selection of the most important annual moisture source regions for the CRB, a threshold was used to delimit these, defined by the value of the 90th percentile calculated from the annual *(E-P)>0* values integrated over the 10 days of transport. This value acts as a boundary to delimit those regions where air masses gain more humidity on their journey to the CRB, representing the 10% of grid points with the highest positive values of *(E-P)i10* on the map. This criterion was applied for similar purposes by Drumond et al. (2014, 2016a, 2016b). The CRB itself is considered a source of moisture, permitting to evaluate its role in the local budget of *(E-P)*. Tracking the air parcels forwards from each of the delimited moisture sources allows us to compare their contributions and thus the importance of each in the total moisture influx to the CRB.

Data for precipitation were obtained from the CRU TS v.3.23 database (Harris et al., 2014) with a spatial resolution of 0.5º. The runoff, the geopotential at 850 hPa, and the vertically integrated moisture flux (northwards and eastwards) form part of the Era Interim Reanalysis Project (Dee et al., 2011), with a resolution of 1ºx1º in latitude and longitude. The corrected monthly mean discharge of the Congo River recorded at the gauging station at Kinshasa (4.0º S, 15.3º E) was provided by the Global Runoff Data Centre (GRDC). To estimate the actual evaporation over the moisture sources we use two state-of-the-art base data sets: OAFLUX and GLEAM. The monthly ocean evaporation data are obtained from the OAFLUX project, which uses surface meteorological fields derived from satellite remote sensing and reanalysis outputs produced from the

NCEP and ECMWF models (Yu et al., 2008). The monthly evaporation from the land is estimated from GLEAM v2 (Global Land Evaporation Amsterdam Model) data, which takes into account a set of algorithms including transpiration, bare-soil evaporation, interception loss, open-water evaporation and sublimation (Miralles et al., 2014), all of which are important considering the dense forests of the CRB.

The selection of global datasets was decided because of documented gaps in the hydrological information of the CRB (Tshimanga, 2012). However, observational data series are available on the SIEREM website (Boyer et al., 2006) mainly to the north part of the basin. In this work, the analysis covers the period 1980-2010 taking into account the availability of ERA-Interim from 1980 and the river discharge data available at Kinshasa gauge station until 2010.

The role of general circulation in the hydrological cycle can be shown clearly through maps of vertically integrated atmospheric moisture flow (Peixoto and Oort, 1992). Also known as Vertically Integrated Moisture Flux (VIMF), this allows readers to compare moisture transport under an Eulerian perspective (Drumond et al., 2014); consequently these maps should lend support to explanations of moisture budget calculated using FLEXPART.

The methodology used to quantify drought or wet conditions in the CRB is based on the Standardized Precipitation Evapotranspiration Index (SPEI), which is a multi-scalar drought index that considers the effect of both precipitation and atmospheric evaporative demand (AED) (Vicente-Serrano et al., 2010). The SPEI for the CRB was calculated at time scales from 1 to 24 months using precipitation and reference evapotranspiration (ETo) obtained from the CRU TS v.3.23 dataset. The criterion of McKee et al. (1993) was used to identify those years of severe and extreme drought and wet conditions (according to the SPEI threshold of +/-1.5). Hydrological drought conditions were quantified at the gauging station of Kinshasa using the Standardized Streamflow Index (SSI) (Vicente-Serrano et al., 2012).

3 Results and Discussion

3.1 Climatology: Rainfall and runoff over the basin and Congo River discharge

The annual cycle of precipitation over the CRB is depicted in Figure 2. The most notable feature of the monthly patterns is the latitudinal migration of the maximum precipitation throughout the year, which leads to different seasonal patterns over the territory (Bultot, 1971; Chishugi 2008). Based on previous results Mahe (1993) defined four great climatic zones over the Congo Basin: the North (Ubangi River Basin), where the influence of the North African continental air mass is prominent; the South (Kasai River Basin), which is influenced by South African air masses; the eastern and south-eastern parts of the basin (Lualaba River Upper Basin), which are influenced by the humid Indian Ocean air masses; and the Center-West, where the climate is controlled by the Atlantic Ocean. In fact, the evaluation of the impact of rainfall on various sectors and its distribution throughout the annual cycle may be as important as the total annual rainfall (Owiti and Zhu, 2012). During January, February, and March, the southern half receives more precipitation, while April is a transitional month with

maximum rainfall in the west-central and northeast parts of the basin. From May to August the rainfall pattern appears homogeneous and reveals that the majority of the average precipitation occurs in the northern part, coinciding with the northward excursion of the ITCZ between February and August (Nicholson and Grist, 2003; Suzuki, 2011). From May to October, the northeast of the CRB receive the highest rainfall, favouring the Oubangui catchment, a right-bank tributary of the Congo River that drains at the Bangui gauge station an area of 488500 km^2 (Runge and Nguimalet, 2005). In September the rainfall increases to the south affecting the centre of the basin, with the greatest extension in October. In November, the central and southwestern parts of the CRB receive more rainfall and during December there is also an extension to the southeast. The regime of precipitation over the CRB is clearly differentiated by a latitudinal oscillation of maximum accumulated values, in accordance with several studies reviewed by Alsdorf et al. (2016) and within an interannual variability higher in the north and south than in the central units of the basin (Mahe, 1993).

Monthly average precipitation for the whole basin shows an annual cycle with two maximum peaks during March-April and October-December, with values greater than 4.5 mm day^{-1}, each accounting for 21% and 32.6% of the mean annual rainfall in the CRB, respectively (Fig. 3). During June and July, the average rainfall reaches its lowest level of around 2 mm day^{-1}. This cycle is similar to that described by Washington et al. (2013), who compared the Congo rainfall climatology through several datasets obtained from reanalysis and ensemble models. However, they argued that the maximum rainfall in the basin occurs from March to May and from September to November, while the minimum occurs in June-August. The differences in monthly average precipitation may be due to the areas used; they used a box region over equatorial west Africa while we use the CRB boundaries.

The mean annual cycle of runoff in the CRB (Fig. 3) follows the same annual cycle as rainfall although it is always lower, varying between maximum values of 3.0 and 3.5 mm day^{-1} during November-March and minimum values below 1.5 mm day^{-1} during July and August. The long-term distribution of precipitation and runoff over the African continent is almost the same (Siam et al., 2013), but the highest values of runoff are concentrated in the heart of the equatorial forest along the Middle Congo River branch (Alemaw, 2012), with these wetlands receiving the majority of their waters from upland runoff (Lee et al., 2011) and several large rivers draining into the Congo in this middle section; the largest of these is the Ubangi, at the north of the Congo Basin (Harrison et al., 2014). The interannual correlation calculated between the two series (precipitation and runoff) over the CRB is high, $r = 0.73$ (significant at $p<0.05$) and $r = 0.72$ with a one-month lag. Fig. 3 shows that from March onwards the runoff reflects a one-month lag compared with precipitation. In general, in a steady state, the precipitation exceeds the evaporation (or evapotranspiration) over the land and the residual water runs off, resulting therefore in a continental freshwater discharge into the oceans (Dai and Trenberth, 2002). This also occurs in the CRB, where monthly values of precipitation minus the actual evapotranspiration obtained from the GLEAM dataset seem to follow the same annual cycle as precipitation (Fig. 3). In June *(P-E)* has a negative value, which means that on average there is more evaporation in the basin than precipitation [as in Dai and Trenberth (2002) and Siam et al. (2013)].

The mean annual discharge of the Congo River is 38617.4 $m^3 s^{-1}$, as calculated from the GRDC monthly discharge values registered at the Kinshasa gauging station in the period 1980-2010. In the secular chronic of the hydro-pluviometric data (1903-2010) recorded at Brazzaville gauge station, close to Kinshasa and analysed by Lareque et al. (2013), the average flow of the Congo River from 1982 to 1994 is below the annual mean, followed by a period of stability from 1995 to 2010. At long-term results of Mahe et al. (2013) pose that as for the equatorial rivers, the Congo river runoff time series (at the Brazzaville station) follows no long-term trend (here these author refers runoff as discharge) and that the minimum shows a lesser inter-annual variability than that of the average or of the maximum.

The annual cycle of discharge (which is very similar to the precipitation and runoff) shows climatological maxima during November-December (Fig. 3) with values above 48000 m^3/s, while in July and August the minimum is less than 30000 m^3/s. Despite this, a difference is seen during March when high precipitation and runoff occur, but the discharge is low. During the next few months the precipitation and runoff decrease while in contrast the discharge increases, reaching a maximum in May. This lag should reflects the time needed for the surface runoff to reach the river mouth but also the groundwater contribution (Dai and Trenberth, 2002, 2008; Marengo, 2005; Rwetabula et al., 2007; Sear et al., 1999), as documented by Materia et al. (2012) using data recorded at Brazzaville station, about 400 km upstream of the river mouth. The direct relationship between precipitation over the basin and the discharge has a correlation of 0.52, which increases to 0.66 for a one-month lag (both statistically significant at $p<0.05$), confirming the lagged response mentioned earlier. Briquet, (1993) pointed out that a translation of the stability of this hydrological regime is shown by a high (low) frequency of floods occurrence on close dates from one year to the other. Future climate projections (21st century) despite to be uncertain, show a basin average increase in both rainfall and evaporation, but the total increase in rainfall tends to be higher than the increase in evaporation and result in most scenarios the runoff is increasing (Beyene et al., 2013). Nevertheless, for the northern sub-basins of the Oubangui and Sangha Rivers Tshimanga and Hughes (2012) downscaled scenarios in which occur more than 10% decrease in total runoff as a consequence of relatively little increase in rainfall and a consistent increase in potential evapotranspiration.

3.2 Identification of the moisture sources

In December, January and February over the CRB, areas of *(E-P)i10>0* (moisture sources) are represented by reddish colours, and are located over the northern half of the CRB and over the river mouth (Fig. 4). Negative values *(E-P)i10<0* (sinks), in blueish colours, cover the southern part of the CRB. Outside the boundaries of the basin, *(E-P)i10>0* values can be seen spread over the northeast of the continent, the Mediterranean Sea, the Red Sea, the Arabian Sea, and the tropical-east South Atlantic Ocean. Negative values are observed in the southeast of the basin, the tropical-west Indian Ocean, and the equatorial Atlantic Ocean around the Equator. For these three months the moisture convergence over central-equatorial Africa between 0º-20ºS, together with a divergence belt to the north of 0º, can be seen. The patterns of atmospheric

divergence and convergence are associated with high-pressure systems as well low pressures at the Equator and in the ITCZ zone, approximately. The deep convection of the ITCZ depends on the contribution of water vapour by the surface moisture flux, supplied as surface latent heat flux, and the horizontal moisture flux in the lower free atmosphere (Suzuki, 2011). The Vertically Integrated Moisture Flux (VIMF) identifies moisture reaching the CRB from divergence zones in the Sahel and the Arabian Sea. It is extremely important to assess the VIMF because in Equatorial Central Africa the seasonal variability of the spatial gradient of precipitation recycling is regulated by both the direction and the strength of the moisture flux (Pokam et al., 2012).

In March the pattern of *(E-P)* changes over the basin, with the establishment of intense moisture sinks located to the centre-west. March seems to be a transitional month, and in April the pattern of *(E-P)* undergoes a more obvious change characterized by moisture loss over the northern half of the basin, a region that acts as a source in the months before this. Despite this, in both months the VIMF remains flowing from east to west over the basin, meanwhile the fields of convergence and divergence of moisture flux are not that different from previous months, instead highlighting a decrease in the divergence over the Arabian Sea (Fig. 4).

Just as in April, from May to September the budget of *(E-P)* over the basin is characterized by negative values in the northern half, in agreement with the maximum precipitation rates for these months (see Fig. 2). Specifically for June to August (the driest months), these values are confined to the northern part of the basin, while an evaporative condition prevails over the rest of the CRB. This demonstrates the ability of FLEXPART to simulate moisture losses in the basin associated with convective precipitation, as well as rainfall migration.

Beyond the CRB, from May to September the source areas *(E-P)i10>0* over the Arabian Sea diminish and the VIMF changes from its previously southwestward direction, which means that moisture transport from this region to Africa is no longer favoured. The *(E-P)i10* patterns are very similar to those of previous months for the other regions. During these months, in the equatorial Indian Ocean, the moisture sinks are less intense than in previous months. At the same time, a latitudinal displacement of moisture convergence and divergence zones occurs over central-equatorial Africa; a joint analysis of the maximum precipitation and convergence of the VIMF provides a rough estimate of the position of the ITCZ (Žagar et al., 2011).

Locations where *(E-P)i10>0* are generally accompanied by moisture flux divergence. However, the Arabian Sea supplies moisture to the CRB from May to October (blueish colour in the left-hand panels); specifically during June-September the VIMF shows an anticyclonic circulation over the Indian Ocean, which induces an intense north-east flow from the Arabian Sea to the Indian Peninsula, in fact, this is an important moisture source for Indian monsoon rainfall (Levine and Turner, 2012).

The sink regions cover almost the whole of the CRB in October and November, when the southeast Atlantic Ocean, the continental regions in the east and north of the basin, and the southwest Indian Ocean all act as moisture sources. A transition of the scheme of moisture source regions takes place in November when once again over the Arabian Sea the *(E-P)i10>0* values appear (Fig. 4). This coincides with the beginning of the summer in the southern hemisphere and the decay phase of the Indian monsoon. The VIMF illustrates the moisture transport from the source regions to an area to the south of 0º in central-equatorial Africa, which enhances the precipitation process over the CRB in accordance with the southward movement of the ITCZ over Africa.

The climatological annual backward average of 10-day integrated *(E-P)* obtained from the Congo River Basin is presented in Figure 5. This figure summarizes the most important moisture sources for the CRB throughout the year. As discussed earlier the boundaries of the moisture sources regions were identified by imposing the 90th percentile (p90) threshold of the annual *(E-P)i10>0* values. This equates to 0.43 mm day^{-1}, denoted in Figure 5 by the dashed lines. Five continental (C) and four oceanic (O) moisture sources were defined (Fig. 6). The five continental regions are located as follows: central and northeastern Africa (C1), centre-west part of the continent on both sides of Equator and at the river mouth (C2), from the river mouth along the Atlantic coast (C3), the east of the CRB extending along the west coast of Africa from the north of Somalia and Ethiopia to approximately 20ºS (C4), and finally the CRB itself. The four oceanic sources are: the Red Sea (O1), the Arabian Sea (O2), the eastern part of the tropical-equatorial South Atlantic Ocean along the coast of Africa (O3), and finally the tropical west Indian Ocean (O4). Moisture source regions are not stationary, varying in intensity from year to year, and expected to change in the future (Gimeno et al., 2013b). In addition, their role may change given the high decadal- and century-scale variability of the African climate (Masih et al., 2014). Nevertheless, these source regions provide insight into the mechanisms by which atmospheric moisture transport takes place towards central equatorial Africa, and how these impact precipitation in the CRB. A combination of factors may influence the role of each in the moisture influx into the CRB, such as the amount of water evaporated, the distance between each source and its target area, the atmospheric circulation, and the residence time of water vapour in the atmosphere.

A comparison with the evaporative moisture sources for the CRB obtained using the quasi-isentropic method and available online (http://cola.gmu.edu/wcr/river/basins.html) confirms the importance of recycling in the CRB, in agreement with our results (Fig. 4, 5). There are nevertheless some differences at the annual scale, in that parts of the northern half of the basin act as moisture sinks (Fig. 5), and that the quasi-isentropic climatology mentioned above considers the entire basin to be an evaporative source. Another clear difference is the Indian Ocean, where our results reflect more clearly the seasonal latitudinal migration of the evaporative regions over the year.

3.3 Freshwater evaporation in the sources

An analysis of the evaporation rate over the moisture sources may support our understanding of their role in the moisture uptake for the CRB over the year. It is most important to note that although the mean evaporation over a region considered to be a moisture source, quantified here using GLEAM and OAFLUX, can be high, its contribution to precipitation over the

CRB might not be because it could be providing moisture for precipitation in other target regions as well. The geographical location of the basin allows it to receive moisture from the Atlantic and Indian Oceans, as well from land regions around the basin, as Fig. 6 shows. Oceanic evaporation is highly important if we consider that evaporation from the ocean surface equates to roughly 84% of the total amount of water evaporated from the planet (Oki, 2005), and the role of the oceans is decisive in continental precipitation (Gimeno et al., 2010). The mean annual evaporation from the sources is given in Table 1 using data from OAFlux and GLEAM for the ocean and continental regions, respectively. On average, O4 and O1 are the most evaporative sources while O3 is the least evaporative. Among the continental sources, the most evaporative are C2, CRB and C3.

Because the sources are located in two different hemispheres, they should have different annual evaporation cycles (Figure 7). From the FLEXPART backward experiment from the CRB, monthly positive values of *(E-P)i10* were calculated over each source (hereafter E-FLEX) to compare over the year the average of evaporation over the sources with the moisture average uptake from each source to the CRB. *(E-P)>0* can be discounted after *(E-P)* has been integrated without altering the general patterns of net precipitation, where *(E-P)>0* is discounted using a monthly or longer time scale (Castillo et al., 2014). In Figure 7 it is possible to observe both series for comparison, E-GLEAM (evaporation data over continental sources) or E-OAF (for oceanic ones) and E-FLEX. On the African continent, in C1 from May to October (boreal summer) E-GLEAM is higher than E-FLEX, and the opposite takes place in the other months, indicating when this source becomes more efficient in providing moisture to the CRB (gray shaded areas in Fig. 7, C1). The next continental source is C2 which shows the higher land annual evaporative value (Table 1). In this source, the annual cycle of E-GLEAM and E-FLEX differs from C1. Over this region, the E-FLEX values are greater than the local evaporation calculated using the GLEAM dataset during February and from June to October (gray shaded areas in Fig. 7, C2). Despite the local evaporation E-GLEAM does not show any great variations over the year, varying from 2 to 3 mm day^{-1}, the E-FLEX shows a bimodal cycle with a minimum in May (~2 mm day^{-1}) when major local evaporation occurs, and a maximum in August (~4.2 mm day^{-1}) when local evaporation is at its lowest. This behaviour illustrates that it is possible to have moisture available in the atmosphere (higher E-GLEAM values) but less humidity is taken up by air masses and then carried towards our target region (lower values of E-FLEX); in this mechanism the rainfall over the region must play a key role since the E-FLEX could be lowest than E-GLEAM as a result of high P values over the region. The gray shaded areas in Figure 7 indicate those months when the transport of moisture is favoured from the source to the CRB. Over the course of several days an air parcel may undergo multiple cycles of evaporation and precipitation (Sodeman, 2008) and in our case, after integrating monthly data over 10 days it is hardly surprising that the E-FLEX values could be greater than local evaporation. Nevertheless, C2 is a land region, where the recycling concept is most useful because moisture for evaporation is limited by precipitation, whereas over the oceans the surface is clearly wet regardless of whether it rains or not (Trenberth, 1999). The C3 source, separated from C2 by the Congo River mouth, follows a similar annual evaporation cycle to C2, but with lower values (<1 mm day^{-1}) during June-October (Fig. 7, C3). In addition, the E-FLEX values are higher than E-GLEAM in February and July-September. In the months of

March-May and November, C3 becomes less efficient at providing moisture to the CRB. For the continental source C4, the annual cycle of local evaporation (E-GLEAM) is similar to C2, C3 but the moisture uptake by air masses tracked backwards from the CRB (E-FLEX) over C4 is always greater than E-GLEAM (unless in February), indicating that this source is very efficient in terms of moisture uptake for the CRB, agreeing with results of van der Ent et al. (2014). For CRB the annual cycle of the E-GLEAM is characterized by maximum values during December-May and minimum in July-August (Fig. 7, CRB). In January-February, April-October, and December, E-FLEX is higher than E-GLEAM, in accordance with the decreasing precipitation over the basin (Fig. 3). This is understandable because the moisture uptake (E-FLEX) over the basin itself must be favoured when the precipitation over it decreases. Comparing the precipitation annual cycle in the CRB (Fig. 3) with E-GLEAM (Fig. 7), it can be seen that both show the same annual cycle, but they show opposite behaviour from E-FLEX (Fig. 7, CRB). This relationship describes a scheme in which the precipitation and evaporation are strongly lineally related; in fact, the evaporation as a source for precipitation over land depends on the availability of surface moisture, which in turn depends upon the disposition of precipitation once it hits the ground (Trenberth, 1999). But, the moisture uptake is the opposite, determining when the source is more effective in providing moisture for itself. This relationship is not strictly interdependent because it could be modulated by moisture income from the other sources or transported outside the boundaries of the target region (the basin).

Regarding the oceanic sources of moisture, in the source O1 the mean annual E-OAF is 4.60 mm day^{-1}. This source is located on the Red Sea, where the oceanic evaporation rate is the highest in the world according to Abdulaziz (2012). After reviewing many studies Sofianos et al. (2002) confirmed several differences in the mean annual evaporation rate for the Red Sea, but it was estimated at around 2.06 m $year^{-1}$ (~5.6 mm day^{-1}). Figure 7 shows the annual cycle of evaporation (E-OAF) in this source, which is characterised by higher values during the boreal winter months and minimum values in summer, in accordance with Bower and Farrar (2015). Monthly E-FLEX values obtained over this source follow the same annual cycle as E-OAF but with lower values. This means that despite to be a high evaporative source, the moisture uptake from O1 to the air masses in transit to the CRB is less than that which it must provide itself to the atmosphere; converting it into a region that is not efficient in terms of the moisture supply to the CRB. In contrast, it seems an important moisture source during December-February over continental areas to its Northeast and during June-August to the remote area of the Indian Peninsula (Gimeno et al., 2010). Located in the Arabian Sea, the O2 source shows two evaporation peaks during December-January and June, and two minima in April and September (Fig. 7). This cycle was also noted by Sadhuram and Kumar (1987), who showed that the maxima are related to strong winds, and the minima are a result of low wind speeds together with weak vapour pressure across the Arabian Sea. The moisture uptake over this source between April-October is almost insignificant, but the evaporation from OAFlux is greater, which means that this source is not efficient in delivering moisture to the CRB, because during these months it instead contributes to the Indian monsoon (Levine and Turner, 2012). In the Atlantic (O3) has the smallest monthly average evaporation rate among all the oceanic sources throughout the year (<1 mm day^{-1}), showing a negligible annual cycle. Materia et al. (2012) determined that the evaporation rate from the ocean surface is

lower due to the fact that part of this oceanic region is affected by the huge freshwater discharge of the Congo River, contributing to a decrease in Sea Surface Salinity (SSS) and Sea Surface Temperature (SST). Despite this, E-FLEX is greater than E-OAF except for during April and May, when the moisture uptake over this source is less than 1 mm day^{-1}. The moisture uptake has two peaks, one in February and the other in September-October. The last oceanic source is O4, the most evaporative and characterized by a maximum average E-OAF in May-July (>5.5 mm day^{-1}) and a minimum at the beginning and end of the year (Fig. 7, O4). This behaviour is in accordance with the results of Yu et al. (2007), who argued that the enhancement of evaporation occurs primarily during the hemispheric winter (defined as the mean of December–February for the northern hemisphere and June-August for the southern). The positive values of E-FLEX over this source (O4) are lower and quite different from the mean E-OAF during all months. This means that on average this source is not very efficient in supplying moisture to the CRB. The efficiency of a region, providing moisture for precipitation at a target area, depends on the amount of evaporated water that reaches it, and not just on the initial evaporation rate. In this mechanism, we must highlight the importance of the atmospheric circulation patterns in determining the water vapour transport, and also, that moisture uptake from each source can be completely different from the evaporation in it.

3.4 Moisture contribution from the sources. Forward analysis.

Having identified the moisture sources regions and their efficient providing moisture to air masses in transient to the CRB, we determined the quantities and locations of the moisture loss over the CRB from those particles leaving each source using forward tracking. For this purpose, a forward experiment with FLEXPART was used, integrating particles forwards over 10 days. FLEXPART was used to compute the changes in *(E-P)* by tracking air parcels regardless of whether it rains or not, but in this case, we computed the result just for those particles arriving in the CRB that lost humidity, hereafter moisture contribution.

Fig. 9 shows the monthly variation in the percentage of moisture contribution to the CRB with respect to the total income and the monthly mean precipitation over the CRB from CRU TS v.3.23 data (Harris et al., 2014). The basin itself turns out to be the most important moisture source throughout the year, contributing more than 55% each month (green line) to the total moisture supply from all the sources to the basin. The contribution from each of the remaining sources does not exceed 20% of the total. This result suggests the importance of moisture recycling over the basin, which differs from the result of van der Ent et al. (2010) who argued that the main source of rainfall in the Congo is moisture evaporating over East Africa, particularly over the Great Lake regions. This is probably a consequence of the method used; their approach takes account of how much of the evaporated water returns as precipitation to the same region (regional evaporation recycling), and what part of it is advected out of the region.

The annual cycle of the percentage moisture supply with respect to the total moisture contribution to the basin is quite similar for the C1 and C3 sources, at less than 4%. C2 and C4 are the most important continental sources (after the CRB itself) supplying moisture for the CRB across the year; they are located to the east and west, respectively, of the basin, and play opposite roles throughout the year. The moisture supply calculated from FLEXPART, $|(E-P)i10<0|$, for C4 follows the

precipitation annual cycle in the basin particularly well. From the oceanic sources, the moisture contributions to the basin from O1 and O2 with respect to the total are less important than those from O3 and O4. It can be seen that the contribution from O3 increases and is thus important when the contribution decreases from the CRB itself, confirming the importance of moisture transport from the Atlantic Ocean. From the Indian Ocean, the contribution of moisture of O4 is at a maximum in January-February and July-August (>15%) when the precipitation rate decreases over the CRB (Fig. 3). The maximum monthly contribution from O4 occurs in April-May (~8%).

We analysed separately the percentage of moisture supplied from land-based and oceanic sources to the total moisture inflow to the CRB for the period 1980-2010. The results confirm that over the whole year near or more than the 80% of the total moisture contribution to the basin origins in land sources, highlighting that more than the 50% of the total comes from the CRB itself (Fig. 10). Evaporation as a source for precipitation over land depends on the availability of surface moisture, which in turn depends upon the disposition of precipitation once it hits the ground (Trenberth 1998). In fact, according to with Eltahir (1998) the soil moisture conditions over any large region should be associated with relatively large boundary layer moist static energy, which favours the occurrence of more rainfall. This hypothesis was also confirmed for West African monsoons by Zheng and Eltahir (1998). In this line van der Ent and Savenije (2011) quantified the spatial and temporal scale of moisture recycling, independent of the size and shape of the region; through this method they found that about the 70% of the precipitation in the center of the South American continent is of terrestrial origin like in many parts of Africa, but specifically in the CRB where occur a strong moisture feedback. For Central Equatorial Africa (CEA) Pokam et al. (2012) and Trenberth (1999) reported a recycling ratio (the fraction of rainfall coming from evapotranspiration and not from moisture advected to the target region) higher than obtained for the Amazon in studies of Eltahir and Bras (1994) and Burde et al., (2006). In the CRB, as already commented the role of forests is also fundamental as they sustain atmospheric moisture through evapotranspiration, which is of utmost importance for the region's water resources, specifically the evergreen forest region (Matsuyama et al., 1994; van der Ent and Savenije, 2011). The key role of continental moisture sources has been also documented for monsoonal wettest regions like the Western Mexico (Bosilovich et al., 2003; Domínguez et al., 2008), Sudamérica (Drumond et al., 2014; Keys et al., 2014) and the Indian region (Misra et al., 2012; Pathak et al., 2015).

The annual role of the moisture sources contributing to precipitation in the CRB is shown in Table 2 as the percentage of the total annual $|(E-P)i10<0|$ amounts over the CRB. The CRB itself is responsible for 59.3% and is the most effective source, followed by C4 with 12%, and O3 with 11.5%. These three sources together account for 82.8% of the total moisture supply to the CRB in the climatological year. The remaining sources contribute 17.2% of the total precipitable moisture. The O1 source, located in the Red Sea, is responsible for just 0.2%.

In order to analyse the joint linear temporal variability, table 3 shows the significant correlation values obtained between monthly series of evaporation, precipitation, runoff in the CRB, river discharge at Kinshasa gauge station and $|(E-P)i10<0|$ from each source over the CRB and the total $|(E-P)i10<0|$ from all the sources (T). All the correlation coefficients are positive and statistically significant at 95%, with the exception of that obtained between $|(E-P)i10<0|$ over the CRB from C2 with the evaporation in the basin and the Congo River discharge at Kinshasa gauge station. As expected, the correlation is greater with precipitation than evaporation as $|(E-P)i10<0|$ may be associated with rainfall process over the CRB. In most of the cases, the initial correlation values with evaporation and those followed obtained with the rest of variables decrease as a consequence of the lagged response of the hydrological system. This behaviour is best appreciated for the correlation with $|(E-P)i10<0|$ over the CRB, obtained in the air masses tracked forward in time from the CRB itself and for the Total contribution. In the correlation values shown in Table 3, $|(E-P)i10<0|$ are best correlated with discharge than with evaporation in the basin, unless for $|(E-P)i10<0|$ obtained in air masses from O4.

Fig. 10 shows the spatial relationship between the moisture supply from the sources and the precipitation over the CRB. The seasonal $|(E-P)i10<0|$ mean values over the CRB are plotted: December-February (DJF), March-May (MAM), June-August (JJA) and September-November (SON). Each map shows the correlation (shown bottom right) of these patterns with the respective climatological precipitation pattern over the basin (not shown).

The moisture sinks for the air masses transported from C1 to the CRB during DJF are more intense (~ -1.5 mm day^{-1}) on a belt located in the central-north part of the basin extending beyond it and to the south (Fig. 10). In MAM the maximum moisture loss moves northwards, and it almost disappears altogether in JJA, while for SON the moisture loss covers the entire CRB with major sinks located in the northern half, in agreement with the high rainfall observed during these months (see Fig. 2). For SON the best correlations were those between the patterns of $|(E-P)i10<0|$ from C1 and precipitation over the CRB (r=0.50). From C2, those sources located to the west of the CRB, the greatest moisture contribution occurs over the west of the basin. In MAM and JJA the $|(E-P)i10<0|$ patterns are observed over the northern half, and the best correlation was obtained for JJA (r=0.63). Contrary to what happens with moisture loss over the basin from C2, the greatest moisture sinks over the CRB for air masses tracked forwards from C3 are mostly positioned to the southwest (best observed for SON and DJF). In MAM and JJA, the sinks are mainly located in the northern half of the basin. From C4 (located to the east of the CRB) the sinks over the CRB decrease in intensity from east to west (the eastern areas show the most intense sinks, >6 mm day^{-1}). It worth remembering that in southern equatorial Africa, and specifically in the CRB region, the precipitation pattern provides a mechanism of atmospheric communication between east and west African´s coasts; these two equatorial regions being generally treated as climatically separate units (Dezfuli et al., 2015). As expected, during SON and DJF (rainiest months) the pattern of $|(E-P)i10<0|$ is more intense. The correlations vary between 0.36 and 0.43, all significant at $p<0.05$. Throughout the year the CRB is the most important moisture source for itself (Fig. 9), which is confirmed by the intensity of the values in the $|(E-P)i10<0|$ patterns (Fig. 10). In DJF and SON greatest moisture sinks (>12 mm day^{-1}) cover the major

part of the centre and south of the basin. In MAM and JJA they are similar to the other sources. The correlation of these patterns with the spatial precipitation was the highest obtained (*r>0.63*).

We previously discussed how the oceanic source O1, despite being an important evaporative region, is not an effective moisture source for precipitation over the CRB. This fact can also be seen in the pattern of $|(E-P)i10<0|$ over the CRB in Fig. 10, where the values are low and oscillate around -0.5 to 0 mm day^{-1}. The pattern also reflects the north-south variability of the precipitation over the year. From the O2 source, located in the Arabian Sea, the greatest moisture contribution occurs in the east and northeast part of the basin, apart from in JJA when the pattern is confined to the northwest and the moisture loss is lower. The O3 source, in the east-tropical Atlantic Ocean, is the most important oceanic source for the CRB, as shown in Table 3. In DJF the major moisture sinks are over the southwest of the basin, in MAM and JJA the moisture loss is mainly over the central and north of the basin, and during SON it is over the east. These patterns show a good correlation with rainfall spatial distribution (*r>0.43*). From O4, located in the West Indian Ocean, the greatest moisture contribution during DJF occurs over the south, and along a longitudinal belt in the central of the basin in MAM; in JJA the major contribution can be detected over the northern part of the basin. During SON when the moisture loss from O4 covers practically the whole territory, with the highest loss over the east, the correlation with the precipitation pattern is negative, however (*r=-0.18*). The highest precipitation for these months shows maxima over the north and west parts, which explains the negative correlation (Fig. 3).

A common characteristic of the $|(E-P)i10<0|$ patterns is that the most intense values are generally located near the moisture sources, as is clear for the contributions from C2, C3, O3, O4, and the CRB itself. The geographic location of the continental sources around the CRB and the dominant atmospheric circulation are the key factors that make this possible.

3.5 The moisture sources role during severe dry and wet periods in the CRB.

We now consider the characteristics of the extreme hydrological conditions seen in the CRB. Central Equatorial Africa (CEA) has experienced a long-term drying trend over the past two decades (Diem et al., 2014, Zhou et al., 2014). In the period 1951-1989 towards Central Africa, the rainfall trend is at first much less clear near the Atlantic Ocean and then becomes more intense towards the interior of the continent (Olivry et al., 1993). It is also noticed in the results of Hua et al. (2016) for Central Equatorial Africa (CEA), who obtained a trend of 0.21 mm d-1 per decade ($p<0.01$) for the period 1979 – 2014 utilizing precipitation data from GPCP.

The temporal evolution of the 1-, 12- month SPEI series for the CRB, shows dry conditions during the periods: 1980-1985, 1992-1998 and 2004-2006, approximately (Fig. 11 a, b). The prevalence of wet conditions can be seen from 1985 to 1991 and from 2007 to 2010. In CEA Hua et al. (2016) documented for April-May-June consistently strong negative anomalies falling since the 1990s, primarily related to SST variations over Indo-Pacific associated with the enhanced and westward extended tropical Walker circulation, which is consistent with the weakened ascent over Central Africa associated with the

reduced low-level moisture transport. Hydrological drought conditions for the Congo River according to Kinshasa gauge station records show temporal consistency with climate drought conditions in the basin (Fig. 11c).

We calculated the monthly correlations between the anomalies of the total moisture influx to the basin $|(E-P)i10<0|$ (summed from all the sources), runoff, and SSI for the 1- to 24- month SPEI time scales (Figure 12) in order to investigate any possible temporal relationships. The significance of the correlation threshold was set at $p<0.05$. The correlations between monthly values of $|(E-P)i10<0|$ and SPEI show significant and high values for all months (Fig. 12a), recorded for short SPEI time scales. The relationship is positive and statistically significant from January to March within the 24 SPEI time scales. During low rainfall climatological months in the basin, especially in June, July and August the correlations become lowest even negative after the SPEI-4.-5 time scales, and generally remain until the last. It indicates a negative feedback that may reflect the increased evapotranspiration modulating the SPEI. As the months advance and the period of less rain ends, the correlations increase being positive and significant during October - December from first SPEI temporal scales until SPEI-10 approximately. In these months for major SPEI, temporal scales correlations become lowest, being also negative as can be appreciated in Figure 12a. However, it changes for January and February when as commented was found positive correlations at all SPEI time scales. This approximately shows a lag of one month needed for the SPEI to reflect wet condition recovery in the CRB.

In Figure 12b the surface runoff seems to be strongly dependent on precipitation deficit for both shorter and annual rainfall deficit. When the rainfall increases over the basin from July to December (Fig. 8), the correlations also increase. Here we observe the same relationship described before between $|(E-P)i10<0|$ and SPEI; but higher correlations were obtained. Correlations between SSI obtained with Kinshasa gauge station discharge and the SPEI (1–24 months) show that the evolution of hydrological conditions is consistent with the meteorological rainfall deficit state over the basin (Figure 12c). In particular, the strongest and most significant correlations were found with SPEI-5 to -7 from January to May, being maximum in April; this suggests the most appropriate time scales to use when identifying the hydrological drought (according to the Congo River discharge at Kinshasa gauge station) in terms of its relationship with the SPEI computed for the whole CRB. From May to July when the precipitation and discharge are minima (Fig. 3) the correlation are negative at first SPEI temporal scales; suggesting a time response of two or three months to reflect SPEI changes at river discharge.

To investigate separately the role of the moisture sources during drought and wet conditions in the CRB we selected a few years affected by severe and extreme conditions. For this purpose SPEI values at the 12-month time scale for December were used to diagnose the status of water balance throughout each year. Moreover, long drought time-scales are generally used to assess streamflow droughts (Svoboda et al., 2012). Besides, at this time scale, it is appropriate to represent the water balance in a region where the precipitation climatology is dictated by latitudinal migration crossing the Equator over the year, such as occurs in the CRB.

During the period 1980-2010, the years 1995 and 1996 were characterized by severe (SPEI12_December = -1.69) and extreme (SPEI12_December= -2.06) drought conditions respectively, while 1982 is characterized as severely wet (SPEI12_December = 1.68). Fig. 13 shows the mean annual contribution from all sources and the anomaly of $|(E-P)i10<0|$ for each event. In 1982 (Fig.13a) the most important moisture contributions are from the basin itself (~120 mm day^{-1}), O3 (~28 mm day^{-1}), and C4 (~27 mm day^{-1}). The anomalies of $|(E-P)i10<0|$ from all the sources are positive, but it is particularly high for the basin itself (18 mm day^{-1}). In 1995 and 1996 (Fig. 13b,c) the greatest moisture loss continues to be that from the air masses from the CRB itself, the oceanic source O3, and the continental C4. However, when the anomalies were analysed all the sources showed negative values, meaning that the moisture support was, in fact, less than the average conditions for the whole period. In 1995 the deficit in the contribution from the CRB and O4 is highlighted. Hua et al. (2016) described how an increase in subsidence across the western edge of Indian Ocean (O4) and a decrease in convection over the Congo Basin (CRB) led to a reduction in moisture transport and rainfall across Central Equatorial Africa. In 1996, a year characterized by extreme drought conditions, the negative anomaly in the moisture supply from all the sources remains, but that computed for the basin is higher than it was in 1995. These results explain a mechanism in which the CRB is more efficient providing moisture for precipitation over itself during wet (dry) periods increase (decrease).

To clarify these results, for the three years under study there was calculated the anomalies of $|(E-P)i10<0|$ (moisture contribution) and $(E-P)i10>0$ (moisture uptake) in air masses tracked forward and backward in time, respectively, from the CRB. It worth noting that utilizing FLEXPART we obtained the budget of $(E-P)$ but not exactly the recycling, which computes the amount of precipitation evaporated falling again within the same region. Besides, to support the results there was calculated the anomaly of the Vertically Integrated Moisture Flux (VIMF) to check the dynamical conditions favourable to the convergence/divergence of moisture flux.

In 1982 a severely wet year, higher positive anomalies of $|(E-P)i10<0|$ are observed in the half north of the CRB, but mostly negative in the south part (Fig. 14a). This pattern is clearly opposite to that obtained for the same year but in the anomalies of $(E-P)i10>0$ for the backward experiment (Fig. 14d), which explains the strengthening role of the half south of the basin as moisture source; mainly favouring the moisture lose over the north part of the CRB, coinciding with the evergreen forest extends. The anomalies of the VIMF support this result, negative values identifying convergence are appreciated over the half north of the CRB, while positive anomalies indicating divergence in the half south (Fig. 15a). During a wet period is supposed that recycling decrease, however, for the Indian region Pathak et al. (2015) described that whereas the monsoon progresses the enhanced soil moisture and vegetation cover leads to increased evapotranspiration and recycled precipitation. Also for the North American Monsoon region, a positive feedback was previously described by Bosilovich et al. (2003), and Domínguez et al. (2008). In 1982 it may happen that in the half north of the CRB increase both the evaporation and precipitation, but the second much more; thus, affecting the budget of $(E-P)$. It was also documented when the tropical

rainbelt shifts northward during boreal summer months; then, the evergreen forest in the CRB gets active rapidly due to the onset of the rainy season, resulting in the increase of evapotranspiration (Matsuyama et al., 1994).

The Oubangui basin in the northeast of the CRB, should have benefited in 1982 due to positive anomalies of $|(E-P)i10<0|$, favouring the precipitation in the half north of the CRB. In the Oubangui basin, a decrease in runoff observed everywhere coincides with a decrease in rainfall with a time lag of 3 years, which can be explained by the sponge-like functioning of the drainage basin, where interannual variability is less important for runoff than for the rainfall series (Orange et al., 1997). An important finding of theses authors is that also the maxima and minima of annual rainfall do not completely coincide with the extreme flow events; as occurred in 1982, a severely wet year when positive anomalies of $|(E-P)i10<0|$ over the half north of the basin including the Oubangui basin. According to the results of Orange et al. (1997), it was documented by Laraque et al. (2013) that from 1982 to 2010 the Oubangui remains in the drought phase, as the Congo returns to a phase of stability.

In 1995 a severely dry year, negative anomalies of $|(E-P)i10<0|$ cover the major part of the basin (Fig. 14b) being more intense over the west and north. Over these areas in the backward analysis are observed positive anomalies of $(E-P)i10>0$ (Fig. 14e) and positive anomalies of the VIMF, indicating the prevalence of divergence (Fig. 15b). In 1996 an extremely dry year, the mechanism is the same like described for 1995 but negative anomalies of $|(E-P)i10<0|$ occupy almost all the basin as well the positive anomalies of $(E-P)i10>0$ does. In the work of Trenberth and Guillemot (1996) are discussed the importance of land surface feedbacks in the 1988 drought and 1993 flood over the United Stated, while results of Dirmeyer and Brubaker, (1999); Bosilovich and Schubert (2001) and Domínguez, et al. (2006) agree that 1988 had a higher recycling ratio than 1993. To resume, in the CRB during dry years 1995 and 1996 prevail positive anomalies of $(E-P)i10>0$; indicating that moisture uptake by the atmosphere predominates. It surely occurs because the evapotranspiration is enhanced and precipitation decrease, but the prevalence of divergence of the VIMF (Fig. 15b,c) does not favour the moisture lose over the basin, which must be transported outside, suggesting the role of the CRB itself as a moisture source for remote regions. A more detailed analysis should be done in future works to determine the role of forests during drought conditions in the CRB. In Figure 12c it's possible to observe, that lowest SSI values obtained for the Kinshasa gauge station discharge data, occur after 1995 and 1996, as commented before due to the lag period from precipitation, runoff and underground water to feed rivers.

An important feature for 1982, 1995 and 1996 is that anomalies of moisture uptake and moisture contribution obtained in air masses tracked backward and forward in time, respectively from the CRB, are not homogenous over the CRB itself. In 1982 and 1995 is best appreciated a relocation of regions sources and sinks of moisture at the basin. This confirms that research on the hydrological cycle should not be developed for the entire basin as a whole, agreeing to Matsuyama et al. (1994). These authors argue that for the CRB the seasonal change of the water budget in the entire basin, can be recognized as the combination of those in the evergreen forest and southern deciduous forest regions, but regional characteristics of the water budget in the basin cannot be explained by studying the basin as a whole.

4. Conclusions

The most important climatological moisture sources for the Congo River Basin have been identified using the Lagrangian model FLEXPART, for a 31-year dataset (1980-2010). To assess the relationship between these sources and the hydrological cycle in the basin the relationship with precipitation, runoff and river discharge at Kinshasa gauging station were all assessed. The mean annual precipitation pattern in the CRB confirms the north-south dipole associated with the annual migration of the ITCZ. On average, maximum rainfall occurs between October and April while minima are observed in June and July, always in good correlation with the runoff and Congo River discharge; in particular the monthly values of discharge have the best correlation (r=0.66) with precipitation having a lag of one month, which is the time taken for the runoff to be seen as freshwater in the Congo River. The backward tracking of air masses reveals that the CRB receives humidity from both hemispheres. At an annual scale, four oceanic sources were identified in the Atlantic Ocean, the Indian Ocean, and the Red Sea, while the continent contains four sources surrounding the CRB, as well as the basin itself, which acts as its own moisture source. The importance of each source in the moisture uptake of the CRB confirms the main role of the CRB on the negative budgets of (E-P) over the basin itself, representing more than 50% of the total moisture loss over the basin supplied by all sources. Hence local recycling processes are hugely important, as pointed out by other authors. Other important sources providing moisture to the CRB are the tropical Atlantic Ocean (O3) and the continental region in the east of the target area (C4). At the same time, the source O1 located on the Red Sea, despite its high evaporation rate, is considered the least efficient source for providing humidity to the basin. Not only does the efficiency of the sources providing moisture to the CRB depend on the evaporation rate, it also influences the amount of water vapour transported to the basin, making the sources more or less effective in terms of precipitation over the CRB. Indeed, the spatial variability of the patterns of $(E\text{-}P)i10<0$ over the CRB after tracking the air masses forwards from all the sources confirms the link between the geographical location of the sources and the location of the greatest moisture sinks over the basin, associated with atmospheric circulation. These patterns show a good spatial correlation with the precipitation distribution over the basin and demonstrate the ability of FLEXPART to reproduce the temporal and spatial variability of the precipitation over the CRB.

The roles of the sources providing moisture during years under extreme and severe conditions confirm the key role of the CRB in modulating the water balance within itself. In wet (dry) years the contribution of moisture from the CRB over itself increases (decreases). As average, the water balance in the atmosphere over the CRB is not homogenous in these years, indicating a distinct role within itself. This confirms that research on the hydrological cycle should not be developed for the entire basin as a whole. The Vertically Integrated Moisture Flux (VIMF) divergence inhibit the precipitation during dry years when moisture uptake is enhanced, which suggest the moisture contribution from the CRB to remote regions, an issue to be investigated in future works. To better understand the complex nature of the hydrological feedback mechanisms in the

Congo River Basin should be performed the identification of moisture sources for the subbasins of the CRB and determine the role in each one. It would provide more accurate information to understand the precipitation variability and the feedbacks of different soil/forest in the water cycle.

The results here obtained will support further studies to address the role of the CRB moisture sources during climate extremes such as flooding, droughts, and extreme river discharge at this basin. One important aspect for consideration in future research is related to the possible influence of Modes of Climate Variability (such as ENSO, SOI, or QBO) on the modulation of moisture transport from these sources to the CRB.

Acknowledgements. This work was supported by EPhysLab (UVIGO-CSIC Associated Unit). R. Sorí would like to acknowledge the grant received by the Xunta of Galicia, Spain, in support of his doctoral research work; R. Nieto acknowledges the support provided by CNPq grant 314734/2014-7 from the Brazilian government; A. Drumond acknowledges the support of the Spanish Government and FEDER via the SETH (CGL2014-60849-JIN) project. Thanks to the IMDROFLOOD project financed by the Water Works 2014 co-funded call of the European Commission.

References

Abdulaziz, S.: Annual and Seasonal Mean Net Evaporation Rates of the Red Sea Water during Jan 1958 – Dec 2007. MSc. thesis, University of Bergen, 2012.

Alemaw, B. F.: Hydrological Modeling of Large Drainage Basins Using a GIS-Based Hybrid Atmospheric and Terrestrial Water Balance (HATWAB) Model. J. of Water Resource and Protection., 4, 516-522, 2012.

Alsdorf, D., Beighley, E., Laraque, Alain., Lee, H., Tshimanga, R., O'Loughlin, F., Mahé, G., Dinga, B., Moukandi, G., and Spencer, R. G. M.: Opportunities for hydrologic research in the Congo Basin. Rev. Geophys., 54, doi:10.1002/2016RG000517, 2016.

Bates, B. C., Kundzewicz, Z.W., Wu, S., and J. P. Palutikof.: Climate Change and Water. Technical Paper of the Intergovernmental Panel on Climate Change, IPCC Secretariat, Geneva, 210 pp., 2008.

Betbeder, J., Gond, V., Frappart, F., Baghdadi, N.N., Briant, G., and Bartholomé, E.: Mapping of Central Africa Forested Wetlands Using Remote Sensing. IEE Journal of selected topics in applied earth observations and remote sensing. 7, 2. 2014.

Beyene T., Ludwig F., Franssen W.: The potential consequences of climate change in the hydrology regime of the Congo River Basin. In: Climate Change Scenarios for the Congo Basin. [Haensler A., Jacob D., Kabat P., Ludwig F. (eds.)]. Climate Service Centre Report No. 11, Hamburg, Germany, ISSN: 2192-4058, 2013.

Bosilovich, M.G. and Schubert, S. D.: Precipitation recycling over the central United States diagnosed from the GEOS-1 data assimilation system, J. Hydrometeorol., 2, 26–35, 2001.

Bosilovich, M.G., Sud, Y.C., Schubert, S.D., and Walker, G.K.: Numerical simulation of the large-scale North American monsoon water sources. J. Geophys. Res., 108, 8614, 2003.

Boyer, J.F., Dieulin, C., Rouche, N., Cres, A., Servat, E., Paturel, J.E., and Mahé, G.: SIEREM: an environmental information system for water resources. Climate Variability and Change—Hydrological Impacts (Proceedings of the Fifth FRIEND World Conference held at Havana, Cuba, November 2006), IAHS Publ. 308, 2006.

Broxton, P.D., Zeng, X., Sulla-Menashe, D., Troch, P.A.: A Global Land Cover Climatology Using MODIS Data. J. Appl. Meteor. Climatol., 53, 1593-1605, 2014.

Bultot, F., 1971. Atlas climatique du bassin congolais. Deuxième partie: les composantes du bilan d'eau ; Institut National pour l'Etude Agronomique du Congo (INEAC). Hors série. 150 p.

Burde, G.I, Gandush, C., Bayarjargal, Y.: Bulk recycling models with incomplete vertical mixing, Part II: precipitation recycling in the Amazon Basin. J Clim 19:1473–1489, 2006.

Briquet, J.P.: Les écoulements du Congo a Brazzaville et la spatialisation des apports, Grands bassins fluviaux, Paris, 22-24 novembre, 27-38, 1993.

Camberlin, P., Janicot, S., and Poccard, I.: Seasonality and atmospheric dynamics of the teleconnection between african rainfall and tropical sea-surface temperature: Atlantic vs. Enso, Int. J. Climatol., 21: 973–1005 (2001). doi: 10.1002/joc.673, 2001.

CARPE.: The Forests of the Congo Basin: A Preliminary Assessment. Central African Regional Program for the Environment, 2005. 34 pp.

Castillo, R., Nieto, R., Drumond, A., Gimeno, L.: Estimating the Temporal Domain when the Discount of the Net Evaporation Term Affects the Resulting Net Precipitation Pattern in the Moisture Budget Using a 3-D Lagrangian Approach, PLoS ONE., 9(6): e99046. doi:10.1371/journal.pone.0099046, 2014.

Chao,Yi., Farrara, J. D., Schumann, Guy., Andreadis, K. M., Moller, D.: Sea surface salinity variability in response to the Congo river Discharge, Continental Shelf Research., 35–45, 2015.

Chen, B., Xu, X. D., Yang, S., and Zhang, W.: Theor Appl Climatol., 110: 423. doi:10.1007/s00704-012-0641-y, 2012.

Chishugi, J. B.: Hydrological modelling of the Congo River basin: a soil-water balance approach. MSc. thesis, University of Botswana, 2008.

Cohen, A.S., Soreghan, M.J., Scholz, C.A.: Estimating the age of formation of lakes: an example from Lake Tanganyika, East African Rift system. Geology., 21, 511-514, 1993.

Coulter, G. W.: Lake Tanganyika and Its Life, Oxford Univ. Press, New York, 1991.

Dai, A.: Increasing drought under global warming in observations and models. Nature Climate Change. 3: 52-58, 2013.

Dai, A., and Trenberth, K. E.: Estimates of Freshwater Discharge from Continents: Latitudinal and Seasonal Variations, J. of Hidrometeorolgy., 3, 660-687, 2002.

Dai, A., Qian, T., and Trenberth, K. E.: Changes in Continental Freshwater Discharge from 1948-2004, J. Climate., 2773-2792, doi: 10.1175/2008JCLI2592.1, 2008.

Dargie, G.C., Lewis, S.L., Lawson, I.T., Mitchard, E.T.A., Page, S.E., Bocko, Y.E., and Ifo, S.A.: Age, extent and carbon storage of the central Congo Basin peatland complex. Nature., 542, 86-90, 2017.

Dirmeyer, P. A., and Brubaker, K. L.: Contrasting evaporative moisture sources during the drought of 1988 and the flood of 1993, J. Geophys. Res., 104, 383–19,397, doi:10.1029/1999JD900222, 1999.

Dirmeyer, P. A., Brubaker, K. L., and DelSole, T.: Import and export of atmospheric water vapor between nations, J. Hydrol., 365, 11–22, doi:10.1016/j.jhydrol.2008.11.016, 2009.

Dominguez, F., Kumar, P., Liang, X., and Ting, M.: Impact of atmospheric moisture storage on precipitation recycling. J. Climate., 19, 1513–1530, 2006.

Domínguez, F., and Kumar, P.: Precipitation Recycling Variability and Ecoclimatological Stability-A Study Using NARR Data. Part II: North American Monsoon Region. J. of Climate., 21, 5187-5203, 2008.

Drumond, A., Marengo, J., Ambrizzi, T., Nieto, R., Moreira, L., and Gimeno, L.: The role of the Amazon Basin moisture in the atmospheric branch of the hydrological cycle: a Lagrangian analysis, Hydrol. Earth Syst. Sci., 18, 2577–2598, doi:10.5194/hess-18-2577-2014, 2014.

Dee, D. P., and 35 co-authors.: The ERA-Interim reanalysis: Configuration and performance of the data assimilation system, Quart. J. R. Meteorol. Soc.. 137, 553-597, doi: 10.1002/qj.828, 2011.

Dezfuli, A. K., Zaitchik, B. F., and Gnanadesikan, A.: Regional Atmospheric Circulation and Rainfall Variability in South Equatorial Africa, J. of Climate., 28, 809-818, doi:10.1175/JCLI-D-14-00333.1, 2015.

Diem, J.E., Ryan, S.J., Hartter, J., and Palace, M.W.: Satellite-based rainfall data reveal a recent drying trend in central equatorial Africa. Climatic Change., 126: 263, 2014. Drumond, A., Marengo, J., Ambrizzi, T., Nieto, R., Moreira, L., Gimeno, L.: The role of the Amazon Basin moisture in the atmospheric branch of the hydrological cycle: A Lagrangian analysis, Hydrol. Earth Syst. Sci., 18, 2577–2598, doi:10.5194/hess-18-2577-2014, 2014.

Drumond, A., Nieto, R., Gimeno, L.: A Lagrangian approach for investigating anomalies in the moisture transport during drought episodes, Cuadernos de Investigación Geográfica., 42, 113-125, doi: 10.18172/cig.2925, 2016a.

Drumond, Anita., Taboada, E., Nieto, R., Gimeno, L., Vicente-Serrano, S. M., López-Moreno, J. I.: A Lagrangian analysis of the present-day sources of moisture for major ice-core sites. Earth Syst. Dynam., 7, 549–558, 2016. doi:10.5194/esd-7-549-2016, 2016b.

Druyan, L. M., and Koster, R. D.: Sources of Sahel Precipitation for Simulated Drought and Rainy Seasons, J. of Climate., 2, 1438-1446, 1989.

Eltahir, E. A. B., and Bras, R. L.: Precipitation recycling, Rev. Geophys., 34, 367–378, doi:10.1029/96RG01927, 1996.

Eltahir, E. A. B., and Gong, C.: Dynamics of Wet and Dry years in West Africa, J. of Climate., 9, 1030-1042, doi:10.1175/1520-0442, 1996.

Gana, M.B., and Herbert, B.: Spatial analysis from remotely sensed observations of Congo basin of east african high land to drain water using gravity for sustainable management of low laying chad basin of central Africa. The International Archives of the Photogrammetry, Remote Sensing and Spatial Information Sciences, Volume XL-1, 2014. ISPRS Technical Commission I Symposium, 17 – 20, November 2014, Denver, Colorado, USA.

Gimeno, L.: Grand challenges in atmospheric science. Front. Earth Sci. 1:1. doi: 10.3389/feart.2013.00001, 2013a.

Gimeno, L., Drumond, A., Nieto, R., Trigo, R. M., and Stohl, A.: On the origin of continental precipitation, Geophysical Research Letters., 37, L13804, doi:10.1029/2010GL043712, 2010.

Gimeno, L., Stohl, A., Trigo, R. M., Dominguez, F., Yoshimura, K., Yu, L., and et al.: Oceanic and terrestrial sources of continental precipitation. Rev. Geophys. 50, RG4003. doi: 10.1029/2012RG000389, 2012.

Gimeno, L., Nieto, R., Drumond, A., Castillo, R., and Trigo, R.: Influence of the intensification of the major oceanic moisture sources on continental precipitation, Geophys. Res. Lett., 40, doi:10.1002/grl.50338, 2013b.

Haensler, A., Saeed, F. and Jacob, D.: Assessment of projected climate change signals over central Africa based on a multitude of global and regional climate projections. In: Climate Change Scenarios for the Congo Basin. [Haensler A., Jacob D., Kabat P., Ludwig F. (eds.)]. Climate Service Centre Report No. 11, Hamburg, Germany, ISSN: 2192-4058, 2013.

Harrison, I.J., Brummett, R., and Stiassny M.L.J.: Congo River Basin. In: The Wetland Book. C.M. Finlayson et al. (eds.). Springer Science+Business Media Dordrecht. 2016. DOI 10.1007/978-94-007-6173-5_92-1.

Harris, I., Jones, P. D., Osborn, T. J. and Lister, D. H.: Updated high-resolution grids of monthly climatic observations – the CRU TS3.10 Dataset, Int. J. Climatol., 34, 623–642. doi:10.1002/joc.3711, 2014.

Hua, W., Zhou, L., Chen, H., Nicholson, S. E., Raghavendra, A., and Jiang, Y.: Possible causes of the Central Equatorial African long-term drought, Environ. Res. Lett., 11, 1-13, 2016.

Hugues, NLOM. J.: The Economic Value of Congo Basin Protected Areas Goods and Services, J. of Sustainable Development., Vol. 4, No. 1, 130-142, 2011.

Haensler, A., Saeed, F. and Jacob, D.: Assessment of projected climate change signals over central Africa based on a multitude of global and regional climate projections, in: Climate Change Scenarios for the Congo Basin. Climate Service Centre Report No. 11, Hamburg, Germany, ISSN: 2192-4058, 2013.

Ilumbe Bayeli Is'ompona, G. (2006). Rapport des Inventaires Multi-ressources a Bobangi. Kinshasa: USAID—Innovative Resources Management.

International Bussines Publications (IBP).: Congo, Land Ownership and Agricultural Laws Handbook. Volume 1, Strategic Information and Regulation. Edition Updated Reprint International Business Publications, Washington, USA, 2015.

Intergubernamental Pannel of Climate Change (IPCC).: Cambio climático 2007: Informe de síntesis. Contribución de los Grupos de trabajo I, II y III al Cuarto Informe de evaluación del Grupo Intergubernamental de Expertos sobre el Cambio Climático, IPCC, Ginebra, Suiza, 2007.

Jackson, B., Nicholson, S. E., and Klotter, D.: Mesoscale convective systems over western equatorial Africa and their relationship to largescale circulation, Mon. Weather Rev., 137, 1272–1294, doi:10.1175/2008MWR2525.1, 2009.

Kadima, E., Delvaux, D., Sebagenzi, S.N., Tack, L., and Kabeya, S.M.: Structure and geological history of the Congo Basin: an integrated interpretation of gravity, magnetic and reflection seismic data. Basin Research., 23, 499–527, 2011.

Keys, P.W., Barnes, E.A., van der Ent, R.J., and Gordon, L.J.: Variability of moisture recycling using a precipitationshed framework. Hydrol. Earth Syst. Sci., 18, 3937–3950, 2014.

Laraque, A., Mahé G., Orange D., and Marieu, B: Spatiotemporal variations in hydrological regimes within Central Africa during the XX century, J. of Hydrology., 245, 104-117, 2001.

Laraque A., Bellanger M., Adele G., Guebanda S., Gulemvuga G., Pandi A., Paturel J.E., Robert A., Tathy J.P. & Yambélé A.: Recent evolution of Congo, Oubangui and Sangha rivers flows / Evolutions récentes des débits du Congo, de l'Oubangui et de la Sangha., Geo-Eco Trop, 37, 1, 93-100, 2013.

Laraque, A., Pouyaud, B., Rocchia, R., Robin, R., Chaffaut, I., Moutsambote, J.M., Maziezoula B., Censier C., Albouy, Y., Elenga, H., Etcheber, H., Delaune, M., Sondag, F., Gasse, F.: Origin and function of a closed depression in equatorial humid zones : the lake Telé in the north Congo., Jo. of Hydrology, 207, 236-253, 1998.

Lau, K.M., and Yang, S.: Walker Circulation, in: Encyclopedia of Atmospheric Sciences, Pyle J, Curry JA, Holton JR (eds). Academic Press: New York, USA, 6pp., 2002.

Lee, H., Edward, R. B., Alsdorf, D., Jung H. C., Shum, C. K., Duan, J., Guo, J., Yamazaki, D., and Andreadis, K.: Characterization of terrestrial water dynamics in the Congo Basin using GRACE and satellite radar altimetry, Remote Sensing of Env., 115, 3530–3538, doi:10.1016/j.rse.2011.08.015, 2011.

Lehner, B., and Grill, G.: Global river hydrography and network routing: baseline data and new approaches to study the world's large river systems. Hydrological Processes., 27, 15, 2171–2186, 2013.

Levine, R. C. and Turner, A. G.: Dependence of Indian monsoon rainfall on moisture fluxes across the Arabian Sea and the impact of coupled model sea surface temperature biases, Climate Dyn., 38, 11-12, pp. 2167-2190, ISSN 0930-7575, 2012.

Lobell, D.B., Bänziger, M., Magorokosho, C., Vivek, B.: Nonlinear heat effects on African maize as evidenced by historical yield trials, Nature Climate Change., 1 (1), 42-45, 2011a.

Lobell, D.B., Schlenker, W., Costa-Roberts, J.: Climate trends and global crop production since 1980, Science., 333 (6042), 616-620, 2011b.

Li, F., and Ramanathan, V.: Winter to summer monsoon variation of aerosol optical depth over the tropical Indian Ocean. J. of Geoph. Res., 107, 4284, doi:10.1029/2001JD000949, 2002.

Mahe G.: Modulation annuelle et fluctuations interannuelles des précipitations sur le bassin versant du Congo. Coll. PEGI/INSU/ORSTOM, Paris, 22-24, Novembre 1993. pp 13-26.

Mahe, G., Lienou, G., Descroix, L., Bamba, F., Paturel, J.E., Laraque, A., Meddi M., Moukolo, N., Hbaieb, H., Adeaga, O., Dieulin C., Kotti F., Khomsi, K.: The rivers of Africa: witness of climate change and human impact on the environnement. Hydrological Processes., 27 (15), 2105-2114, 2013.

Marengo, J. A.: The characteristics and variability of the atmospheric water balance in the Amazon basin: Spatial and temporal variability, Climate Dyn., 24, 11-22, 2005.

Masih, I., Maskey, S., Mussá, F. E. F., and Trambauer, P.: A review of droughts on the African continent: a geospatial and long-term perspective, Hydrol. Earth Syst. Sci., 18, 3635–3649, doi:10.5194/hess-18-3635-2014, 1014.

Materia, S., Gualdi, S., Navarra, A., and Terray, L.: The effect of Congo River freshwater discharge on Eastern Equatorial Atlantic climate variability, Climate Dyn., 39, 2109–2125, doi:10.1007/s00382-012-1514-x, 2012.

Marquant, B., Mosnier, A., Bodin, B., Dessard, H., Feintrenie, L., Molto, Q., Gond, V., and Bayol, N.: Importance des forêts d'afrIque centrale. In: Les forêts du bassin du Congo - Forêts et changements climatiques. Eds: de Wasseige C., Tadoum M., Eba'a Atyi R. et Doumenge C. Weyrich. Belgique. 128 p. Chapter 1. p. 17-36.

Matari, E.E.: Impacts of Congo convection on tropical Africa's circulation, rainfall and resources, MSc. Thesis, University of Zululand, South Africa, 165 pp., 2002.

Sorre M.: Le climat écologique de la cuvette centrale congolaise [D'après Mr Etienne Bernard]. In: Annales de

Géographie, 57, 305, 73-75, 1948. doi : 10.3406/geo.1948.12165.

Nieto, R., Gimeno, L., and Trigo, R. M.: A Lagrangian identification of major sources of Sahel moisture, Geophys. Res. Lett., 33, L18707, doi:10.1029/2006GL027232, 2006.

Nicholson, S. E., and Grist, J. P.: The seasonal evolution of the atmospheric circulation over West Africa and Equatorial Africa, J. Clim., 16, 7, 1013–1030, 2003.

Nieto, R., Gallego, D., Trigo, R. M., Ribera, P., and Gimeno, L.: Dynamic identification of moisture sources in the Orinoco basin in equatorial South America, Hydrol. Sci. J., 53, 602–617, 2008.

Numaguti, A.: Origin and recycling processes of precipitating water over the Eurasian continent: Experiments using an atmospheric general circulation model, J. Geophys. Res., 104, 1957–1972, 1999.

Orange, D., Wesselink, A., Mahé, G., and Feizouré, C. T.: The effects of climate changes on river baseflow and aquifer storage in Central Africa, in: Sustainability of Water Resources Under Increasing Uncertainty, edited by D. Rosbjerg et al., IAHS Publ., 240, 113–123, Rabat, 1997.

Owiti, Z., and Zhu, W.: Spatial distribution of rainfall seasonality over East Africa, J. of Geography and Regional Planning., 5 (15), 409-421, doi:10.5897/JGRP12.027, 2012.

Peixoto, J. P., and Oort, A. H.: Physics of Climate. AIP-Press, New York, NY: Springer–Verlag New York Press, 1992.

Pokam, W. M., Djiotang, L. A. T., and Mkankam, F. K.: Atmospheric water vapor transport and recycling in Equatorial Central Africa through NCEP/NCAR reanalysis data, Climate Dyn., 38, 1715–1729, doi:10.1007/s00382-011-1242-7, 2012.

Rwetabula, J., De Smedt, F., and Rebhun, M.: Prediction of runoff and discharge in the Simiyu River (tributary of Lake Victoria, Tanzania) using the WetSpa model, Hydrol. Earth Syst. Sci. Discuss., 4, 881-908, 2007.

Pokam, W. M., Djiotang, L. A. T.; and Mkankam, F. K.: Atmospheric water vapor transport and recycling in Equatorial

Central Africa through NCEP/NCAR reanalysis data., Climate Dyn, 38, 1715–1729, 2012.

Potapov, P.V., S.A. Turubanova, M.C. Hansen, B. Adusei, M. Broich, A. Altstatt, L. Mane, and C.O. Justice, 2012: Quantifying forest cover loss in Democratic Republic of the Congo, 2000-2010, with Landsat ETM+ data. Remote Sensing of Environment, 122, 106-116.

Robert, M.: Le Congo physique. ed. 3 Vaillant-Carmanne, Liège. 449 pp, 1946.

Runge, J., and Nguimalet C.-R.: Physiogeographic features of the Oubangui catchment and environmental trends reflected in discharge and floods at Bangui 1911–1999 Central African Republic. Geomorphology., 70, 311–324, 2005.

Salih, A. A. M., Zhang, Q., and Tjernström, M.: Lagrangian tracing of Sahelian Sudan moisture sources, J. Geophys. Res. Atmos., 120, 6793–6808, doi:10.1002/2015JD023238, 2015.

Samba, G., and Nganga, D.: Rainfall variability in Congo-Brazzaville: 1932–2007, Int. J. Climatol., 32: 854-873, doi:10.1002/joc.2311, 2012.

Secretariat of the Convention on Biological Diversity and Central African Forests Commission (SCBD-CAFC).: Biodiversity and Forest Management in the Congo Basin, Montreal, 2009.

Sear, D. A., Armitage, P. D., and Dawson, F. H.: Groundwater dominated rivers, Hydrol. Process., 13, 255-276, 1999.

Siam, M. S., Marie-Estelle, D., and Elfatih A. B. E.: Hydrological Cycles over the Congo and Upper Blue Nile Basins: Evaluation of General Circulation Model Simulations and Reanalysis Products, J. Climate., 26, 22, 8881–8894, 2013.

Sodemann, H., Schwierz, C., and Wernli, H.: Interannual variability of Greenland winter precipitation sources: Lagrangian moisture diagnostic and North Atlantic Oscillation influence, J. Geophys. Res., 113, D03107, doi:10.1029/2007JD008503, 2008.

Sofianos, S. S., Johns, W. E., and Murray, S. P.: Heat and freshwater budgets in the Red Sea from direct observations at Bab el Mandeb. Deep Sea Research Part II: Topical Studies in Oceanography, 49 (7-8):1323–1340, 2002.

Stohl, A., and James, P.: A Lagrangian analysis of the atmospheric branch of the global water cycle. Part I: Method description, validation, and demonstration for the August 2002 flooding in central Europe, J. Hydrometeorol., 5, 656–678, doi:10.1175/1525-7541(2004)005<0656: ALAOTA>2.0.CO;2, 2004.

Stohl, A., and James, P.: A Lagrangian analysis of the atmospheric branch of the global water cycle. Part II: Moisture transports between the Earth's ocean basins and river catchments, J. Hydrometeorol., 6, 961–984, doi:10.1175/JHM470.1, 2005.

Suzuki, T.: Seasonal variation of the ITCZ and its characteristics over central Africa, Theor Appl Climatol., 103:39–60, doi: 10.1007/s00704-010-0276-9, 2011.

Svoboda, M., Hayes, M., and Wood, D.: Standardized Precipitation Index User Guide, World Meteorological Organization, Geneva, WMO Rp. 1090, 24 pp., 2012.

Tshimanga, R. M., Hydrological uncertainty analysis and scenario based streamflow modelling for the Congo River Basin, Ph.D. Thesis, Rhodes University repository. South Africa, 2012.

Tshimanga, R. M., and Hughes, D. A.: Climate change and impacts on the hydrology of the Congo Basin: the case of the northern sub-basins of the Oubangui and Sangha Rivers. Physics and Chemistry of the Earth., 50-52, 72–83, 2012.

Tchatchou B, Sonwa DJ, Ifo S et Tiani AM. 2015. Déforestation et dégradation des forêts dans le Bassin du Congo: État des lieux, causes actuelles et perspectives. Papier occasionnel 120. Bogor, Indonesie: CIFOR. ISBN 978-602-1504-69-7.

Tan, Ch., Yang, J., and Li, Man.: Temporal-Spatial Variation of Drought Indicated by SPI and SPEI in Ningxia Hui Autonomous Region, China, Atmosphere., 6, 1399-1421, doi:10.3390/atmos6101399, 2015.

The Center for Ocean-Land-Atmosphere Studies: http://cola.gmu.edu/wcr/river/, last access 02 February 2017.

Trenberth, K. E.: Atmospheric Moisture Recycling: Role of Advection and Local Evaporation, J. of Climate., 12, 1368-1380, 1999.

Tsalefac, M., François Hiol Hiol, Gil Mahé, Alain Laraque, Denis Sonwa, Paul Scholte , Wilfried Pokam, Andreas Haensler, Tazebe Beyene, Fulco Ludwig, François K Mkanka, Viviane Manetsa, Djoufack, 2015. Climate of central Africa: past, future evolution and its relevance to watershed. In Les forêts du bassin du Congo - Forêts et changements climatiques. Eds: de Wasseige C., Tadoum M., Eba'a Atyi R. et Doumenge C. Weyrich. Belgique. 128 p. Chapter 2. p. 37-52.

van der Ent R. J., and Savenije H. H. G.: Length and time scales of atmospheric moisture recycling. Atmos. Chem. Phys., 11, 1853–1863, 2011.

van der Ent, R. J., Savenije, H. H. G., Schaefli, B., and Steele-Dunne, S. C.: Origin and fate of atmospheric moisture over continents, Water Resour. Res., 46, 1-12, doi:10.1029/2010WR009127, 2010.

van der Ent, R. J., Wang-Erlandsson, L., Keys, P. W., and Savenije, H. H. G.: Contrasting roles of interception and transpiration in the hydrological cycle – Part 2: Moisture recycling. Earth Syst. Dynam., 5, 471–489, doi:10.5194/esd-5-471-2014, 2014.

Vicente-Serrano, S.M., Beguería, S., López-Moreno, J. I.: A Multiscalar Drought Index Sensitive to Global Warming: The Standardized Precipitation Evapotranspiration Index, J. of Climate., 23, 1696-1718, doi: 10.1175/2009JCLI2909.1, 2010.

Vicente-Serrano, S. M., López-Moreno, J. I., Santiago, B., Lorenzo-Lacruz, J., Azorin-Molina, C., and Morán-Tejeda, E.: Accurate computation of a streamflow drought index., J. of Hyd. Eng., 17: 318-332, 2012.

Viste, E., and Sorteberg, A.: The effect of moisture transport variability on Ethiopian summer precipitation, Int. J. Climatol., 33: 3106–3123, doi:10.1002/joc.3566, 2013.

Wang, Q., Wu, J., Lei, T., He, B., Wu, Z., Liu, M., Mo, X., Geng, G., Li, X., Zhou, H., and Liu, D.: Temporal-spatial characteristics of severe drought events and their impact on agriculture on a global scale, *Quat. Int.*, 349, 10–21, 2014.

Washington, R., James, R., Pearce, H., Pokam, W. M., Moufouma-Okia, W.: Congo Basin rainfall climatology: can we believe the climate models?, Phil. Trans. R. Soc. B., 368, 20120296, doi:10.1098/rstb.2012.0296, 2013.

Wasseige, C., M. Marshall, G. Mahé et A. Laraque. 2015. Interactions between climate charateristics and forest. In Les forêts du bassin du Congo - Forêts et changements climatiques. Eds: de Wasseige C., Tadoum M., Eba'a Atyi R. et Doumenge C. Weyrich. Belgique. 128 p. Chapter 3. p. 53-64.

Wesselink A.J., Orange D., Feizoure C.T., Randriamiarisoa, 1996. Les régimes hydro climatiques et hydrologiques d'un bassin versant de type tropical humide: l'Oubangui (République centrafricaine), L'hydrologie tropicale: géoscience et outil pour le développement (Actes de la conférence de Paris, mai 1995), IAHS Publ. N°238, pp 180-194.

Yu, L.: Global Variations in Oceanic Evaporation (1958–2005): The Role of the Changing Wind Speed, J. of Climate.. 20, 5376-5390, doi: 10.1175/2007JCLI1714.1, 2007.

Zhou, L., Tian , Y., Myneni, R. B., Ciais, P., Saatchi, S., Liu, Y. Y., Piao, Shilong., Chen, H., Vermote, E. F., Song, C., Hwang, T.: Widespread decline of Congo rainforest greenness in the past decade, Nature., 86, VOL:509, doi:10.1038/nature13265, 2014.

Table 1. Mean annual Evaporation rate over the sources. Data for the continent were obtained from GLEAM and for the ocean from OAflux.

	Evaporation rate (mm day^{-1})								
Sources	C1	C2	C3	C4	CRB	O1	O2	O3	O4
	1.0	2.5	1.6	1.5	2.4	4.6	1.1	0.71	4.7

Table 2. Moisture contribution from the sources to the CRB (%).

	(E-P)i10<0 in %								
Sources	C1	C2	C3	C4	CRB	O1	O2	O3	O4
	2.3	6.8	2.1	**12.0**	**59.3**	0.2	1.8	**11.5**	4.1

Table 3. Significant monthly correlation ($p<0.05$) between the precipitation from CRU, Runoff from ERA-Int, River discharge from the GRDC and evaporation from GLEAM or OAFLUX, and series of $|(E-P)i10<0|$ forward-integrated using FLEXPART from the sources over the CRB, and with the total $|(E-P)i10<0|$ amount (T). Period used: 1980 – 2010.

	C1	C2	C3	C4	CRB	O1	O2	O3	O4	T
Evaporation	0.35		0.35	0.36	0.37	0.35	0.43	0.14	0.35	0.36
Precipitation	0.60	0.53	0.65	0.77	0.80	0.36	0.58	0.60	0.58	0.83
Runoff	0.66	0.43	0.72	0.69	0.75	0.59	0.73	0.59	0.43	0.75
Discharge	0.49		0.59	0.53	0.54	0.47	0.55	0.33	0.12	0.53

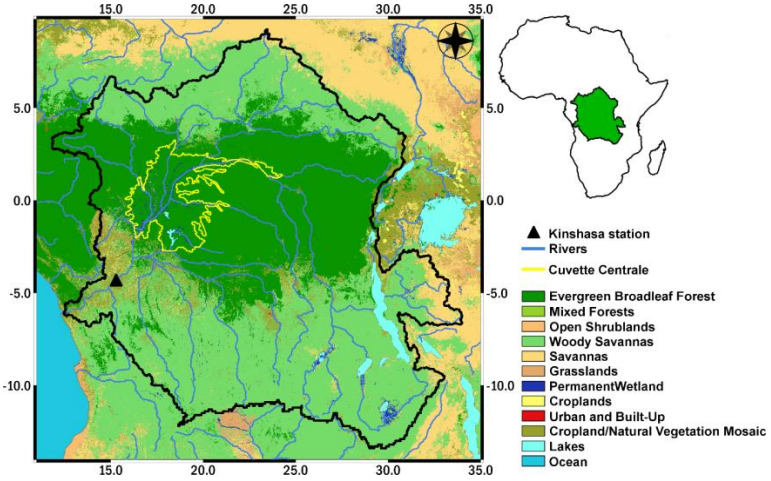

Figure 1. Geographic location of the Congo River Basin showing the Kinshasa gauging station, the fluvial system and the land use based on 10 years (2001-2010) (source: Broxton et al., 2014). The boundaries of the Cuvette Centrale is contoured in yellow (adapted from: Betbeter et al., 2014).

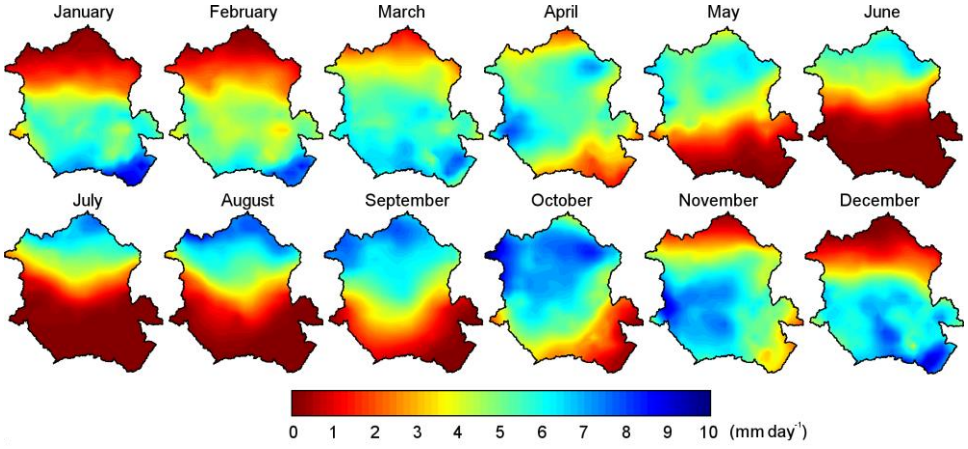

Figure 2. Monthly mean precipitation over the CRB for 1980-2010. Data from CRU TS v.3.23.

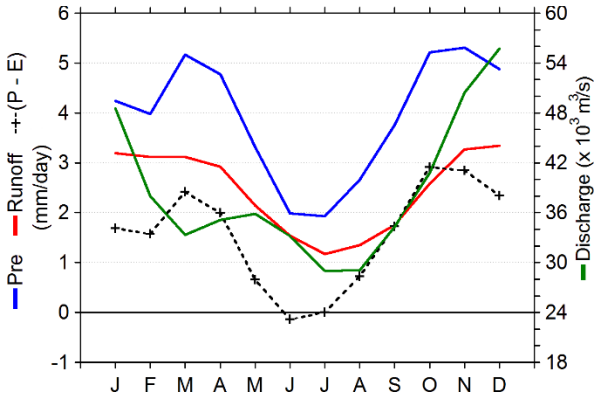

Figure 3. Annual cycle of precipitation, runoff and *(P-E)* in the CRB (left axis), and the Congo River discharge (right axis). Data obtained from CRU, ERA-Int, GLEAM and Global Runoff Data Center, respectively.

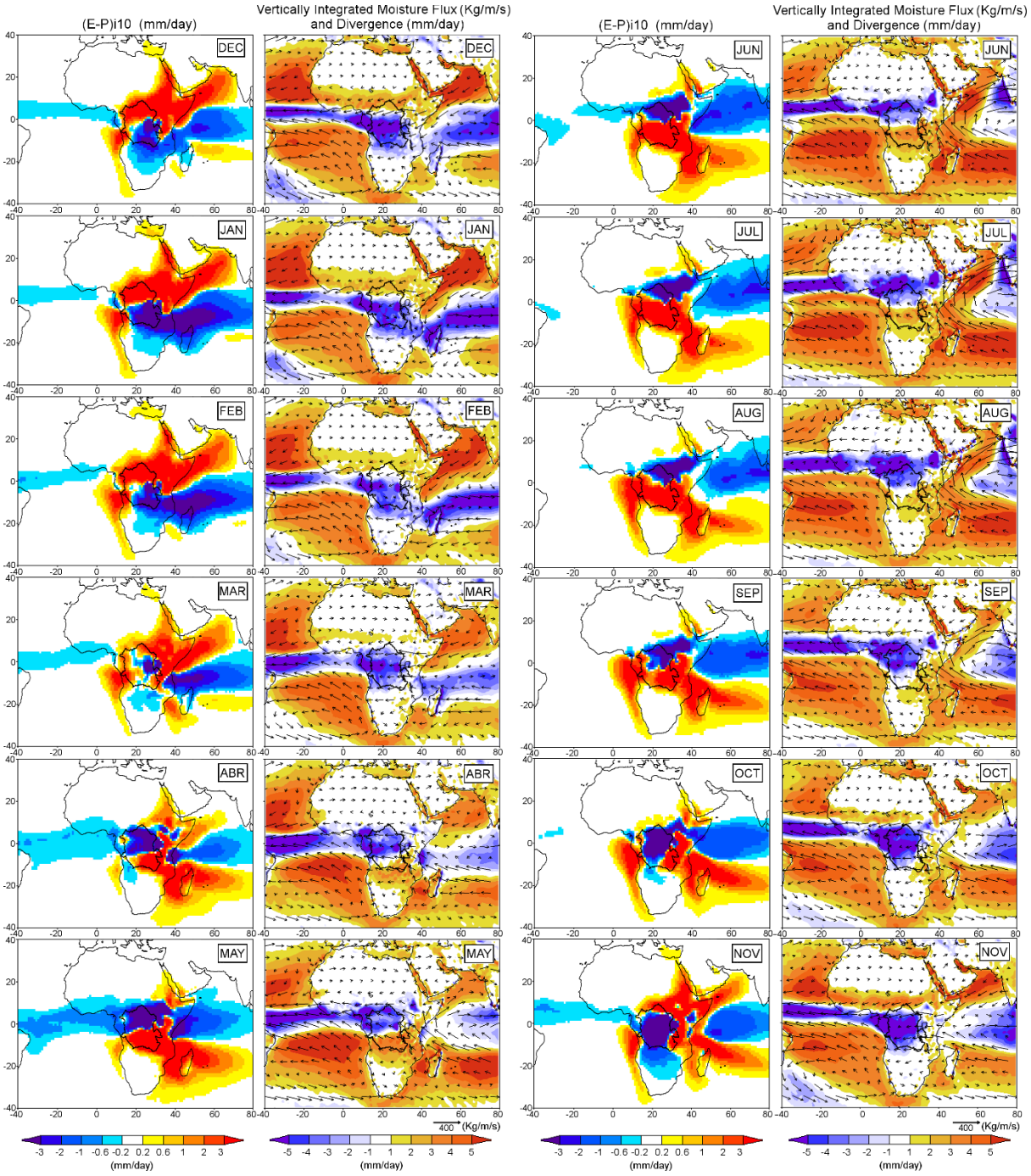

Figure 4. Monthly climatological (E-P) values integrated backwards over 10 days (mm day^{-1}) alongside Vertically Integrated Moisture Flux (kg/m/s) and divergence-convergence (reddish-blueish colours) (mm day^{-1}). Period 1980 - 2010.

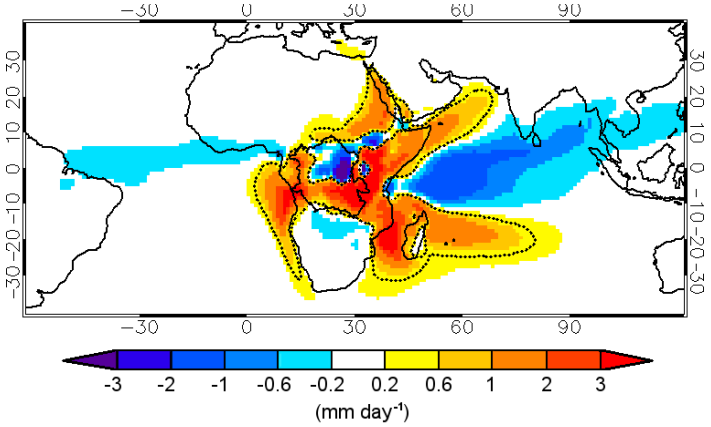

Figure 5. Annual mean values of *(E-P)i10* backward-integrated over 10 days for the period 1980-2010. Dashed lines represent the boundaries of the sources of moisture, defined as p90= 0.4 mm day^{-1}.

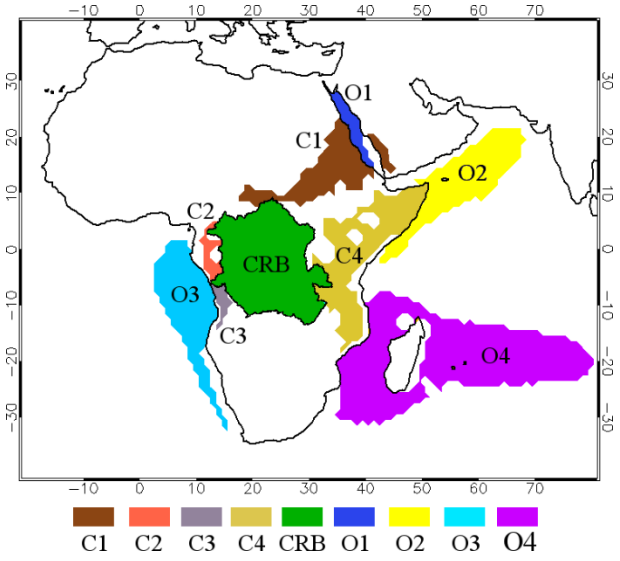

Figure 6. Continental moisture sources for CRB: C1, C2, C3, C4, and the CRB itself; Oceanic moisture sources: O1, O2, O3, and O4.

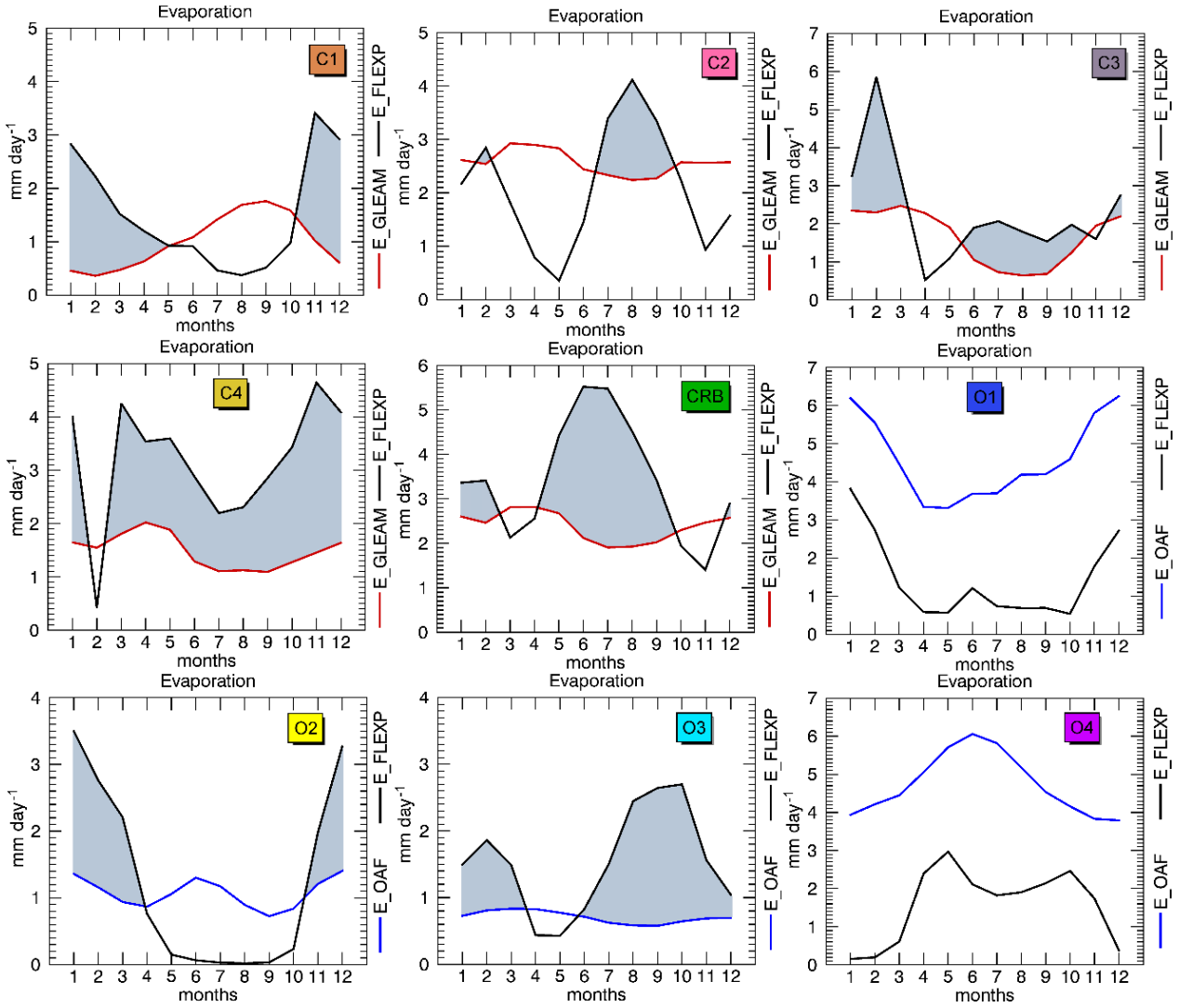

Figure 7. Monthly mean evaporation in continental (C) and oceanic (O) sources (in mm day^{-1}). Data from GLEAM (red lines) and OAFlux (blue lines). E-FLEX: evaporation values over the sources obtained using FLEXPART (black lines). Areas shaded in gray identify where E-FLEX > Evaporation. Data period: 1980-2010.

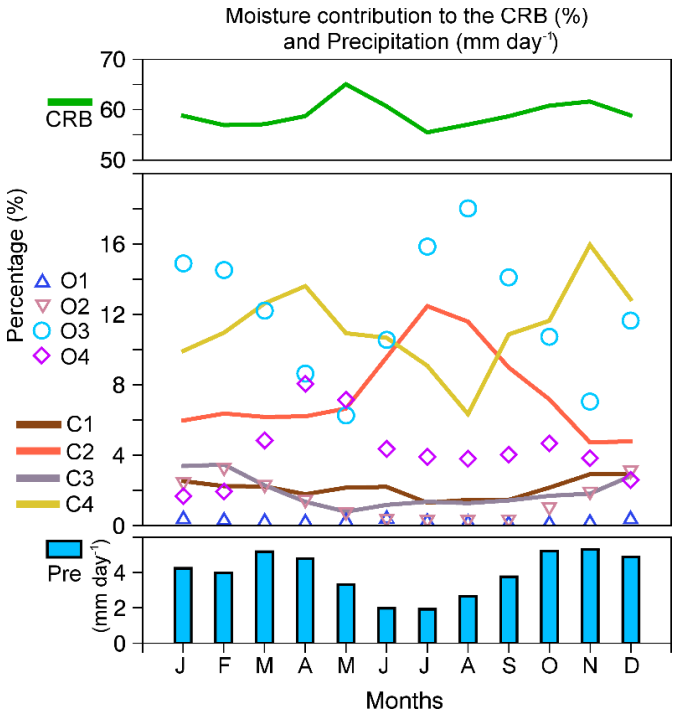

Figure 8. Monthly percent of moisture loss calculated as |*(E-P)i10<0*| forward-integrated from each source over the CRB over 10 days of transport, and monthly mean precipitation from CRU datasets for the period 1980-2010.

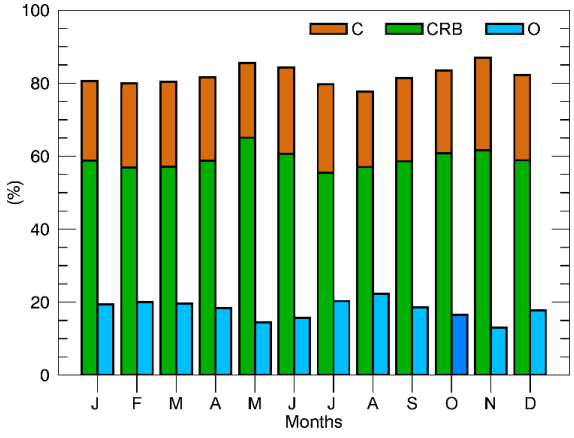

Figure 9. Monthly percentage moisture contributions to the CRB from continental sources (red bars), the CRB itself (green bars), and oceanic sources (blue bars). Data from FLEXPART for the period 1980-2010.

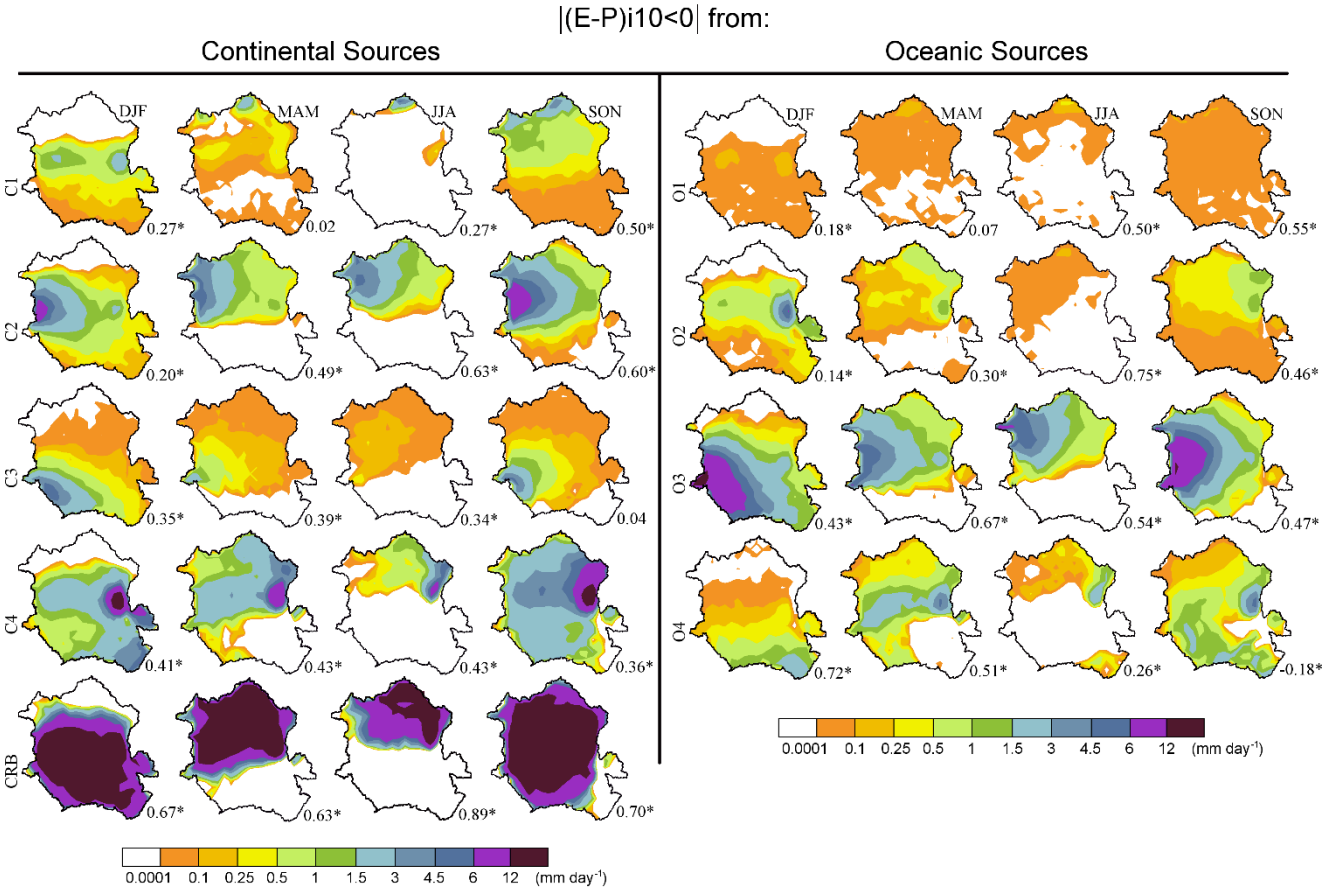

Figure 10. Seasonal mean *|(E-P)i10<0|* integrated forwards from the moisture sources over the CRB, in mm day^{-1}. The number in the bottom-right corner of each plot indicates the correlation with the mean precipitation pattern (asterisks indicate significant values at $p<0.05$). Period 1980- 2010.

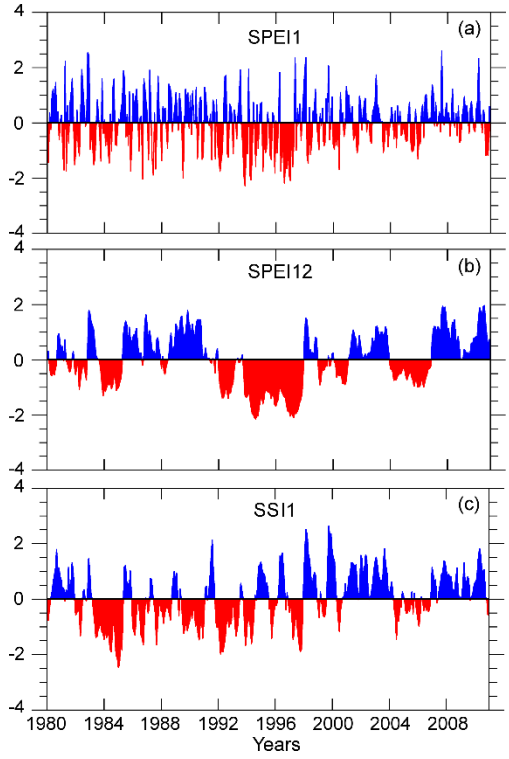

Figure 11. Time evolution of the SPEI in the Congo River basin at 1 (a), and 12 months (b) and Standardized Streamflow Index (SSI) (c) computed for the Congo River discharge. Period 1980 – 2010.

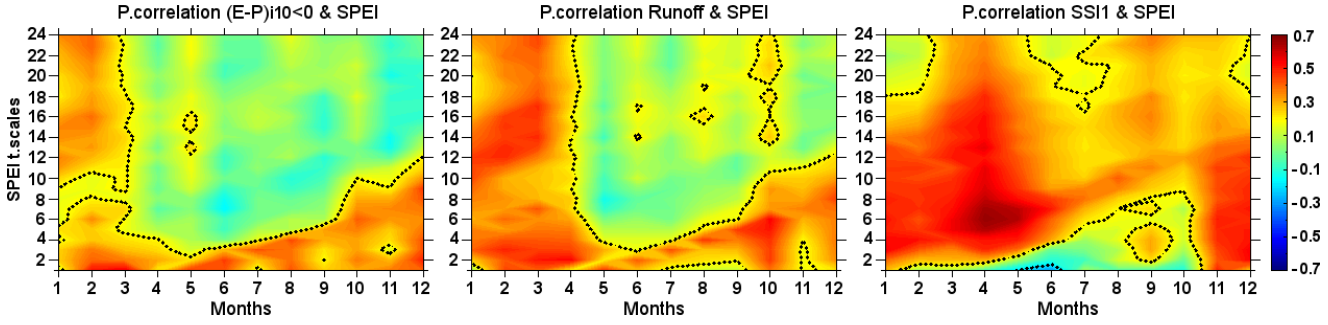

Figure 12. Monthly correlations between |*(E-P)i10<0*|, runoff and SSI with SPEI-1 to SPEI-24 in the Congo River Basin. Dotted lines represent significant correlations at *p<0.05*.

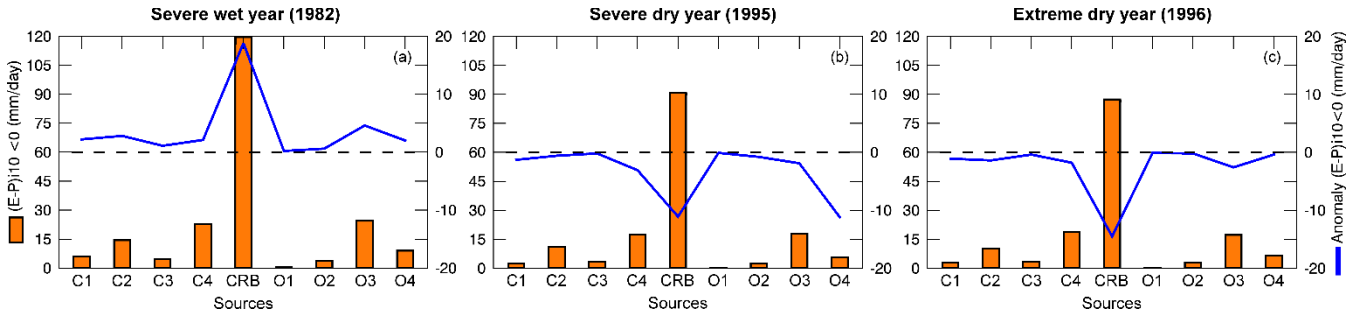

Figure 13. Mean annual moisture contribution from the sources to the CRB (orange bars) during 1982 (severe wet conditions, a), 1995 (severe dry conditions, b) and 1996 (extreme dry conditions, c), and the corresponding anomaly (blue line).

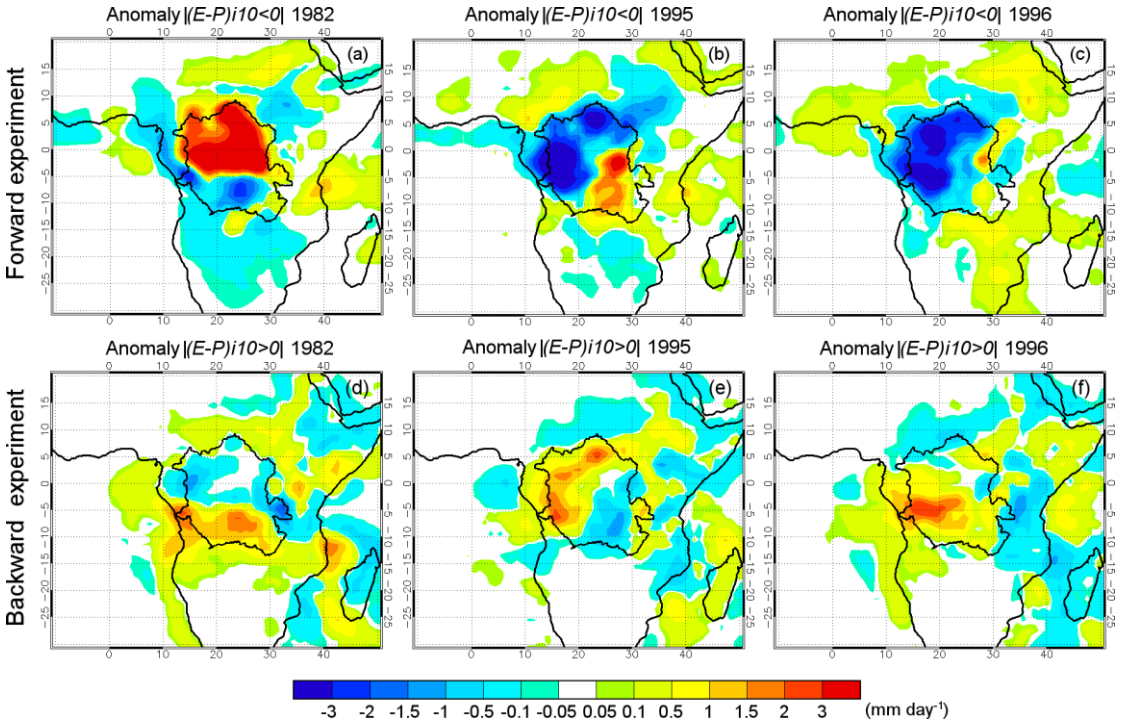

Figure 14. Anomaly of the $|(E-P)i10<0|$ (mm day^{-1}) integrated forwards from the Congo River basin itself during 1982 (severe wet year, a), 1995 (severe dry year, b) and 1996 (extreme dry year, c). Anomaly of the $|(E-P)i10>0|$ (mm day-1) integrated backwards from the Congo River basin itself during (severe wet year, d), 1995 (severe dry year, e) and 1996 (extreme dry year, f).

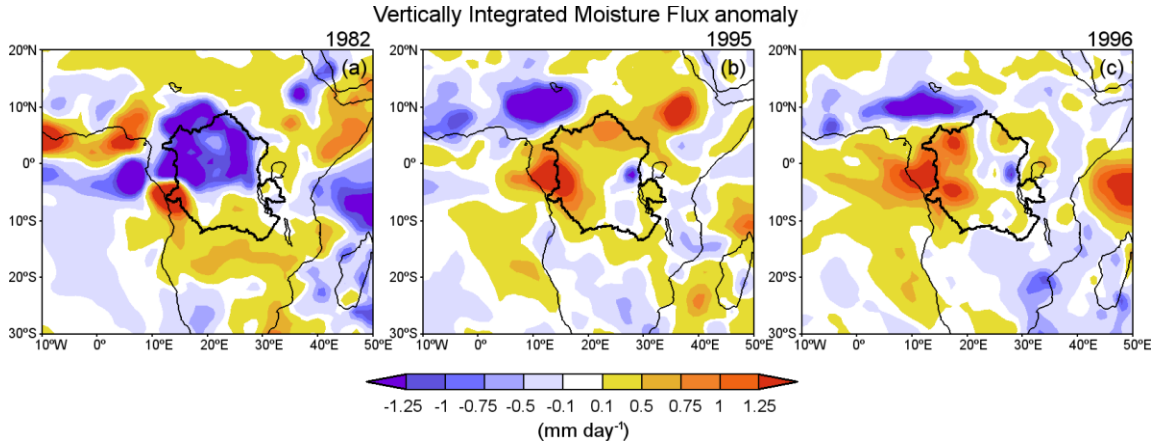

Figure 15. Anomaly of the Vertically Integrated Moisture Flux (VIMF) during 1982 (severe wet year, a), 1995 (severe dry year, b) and 1996 (extreme dry year, c).